



University of Kentucky
UKnowledge

Theses and Dissertations--Electrical and
Computer Engineering

Electrical and Computer Engineering

2012

IMPROVEMENT OF SILICON OXIDE QUALITY USING HEAT TREATMENT

Lei Han

University of Kentucky, lei.han@uky.edu

[Right click to open a feedback form in a new tab to let us know how this document benefits you.](#)

Recommended Citation

Han, Lei, "IMPROVEMENT OF SILICON OXIDE QUALITY USING HEAT TREATMENT" (2012). *Theses and Dissertations--Electrical and Computer Engineering*. 5.
https://uknowledge.uky.edu/ece_etds/5

This Master's Thesis is brought to you for free and open access by the Electrical and Computer Engineering at UKnowledge. It has been accepted for inclusion in Theses and Dissertations--Electrical and Computer Engineering by an authorized administrator of UKnowledge. For more information, please contact UKnowledge@lsv.uky.edu.

STUDENT AGREEMENT:

I represent that my thesis or dissertation and abstract are my original work. Proper attribution has been given to all outside sources. I understand that I am solely responsible for obtaining any needed copyright permissions. I have obtained and attached hereto needed written permission statements(s) from the owner(s) of each third-party copyrighted matter to be included in my work, allowing electronic distribution (if such use is not permitted by the fair use doctrine).

I hereby grant to The University of Kentucky and its agents the non-exclusive license to archive and make accessible my work in whole or in part in all forms of media, now or hereafter known. I agree that the document mentioned above may be made available immediately for worldwide access unless a preapproved embargo applies.

I retain all other ownership rights to the copyright of my work. I also retain the right to use in future works (such as articles or books) all or part of my work. I understand that I am free to register the copyright to my work.

REVIEW, APPROVAL AND ACCEPTANCE

The document mentioned above has been reviewed and accepted by the student's advisor, on behalf of the advisory committee, and by the Director of Graduate Studies (DGS), on behalf of the program; we verify that this is the final, approved version of the student's dissertation including all changes required by the advisory committee. The undersigned agree to abide by the statements above.

Lei Han, Student

Dr. Zhi Chen, Major Professor

Dr. Zhi Chen, Director of Graduate Studies

IMPROVEMENT OF SILICON OXIDE QUALITY USING HEAT TREATMENT

THESIS

A thesis submitted in partial fulfillment of the
requirements for the degree of Master of Science in Electrical Engineering
in the College of Engineering
at the University of Kentucky

By

Lei Han

Lexington, Kentucky

Directors: Dr. Zhi Chen, Professor of Electrical Engineering Department

Lexington, Kentucky

2012

Copyright © Lei Han 2012

ABSTRACT OF THESIS

IMPROVEMENT OF SILICON OXIDE QUALITY USING HEAT TREATMENT

In decades, the tremendous development of integrated circuits industry could be mostly attributed to SiO₂, since its satisfactory properties as a gate dielectric candidate. The effectivity of SiO₂ has been challenged since dielectric layer was scaled down below 3nm, when the gate leakage current of SiO₂ became unacceptable. Institution to silicon-based CMOS techniques were proposed, but they have their own limitations. Nowadays, materials with high dielectric constants are mainstream gate dielectric materials in industry, but a SiO₂ interfacial layer is still necessary to avoid gap between gate dielectric layer and Si substrate, and to minimize interface trap charges. In this thesis work, by applying lateral heating process on Si wafer with thermally grown ultrathin SiO₂, the gate leakage current density could be reduced by 3-5 order of magnitude. MOS capacitors were fabricated, and electrical properties were tested with semiconductor parameter analyzer and LCR meter. The underlying mechanism of this appealing phenomenon was explored. Since unacceptable gate leakage current is one of the main reasons which prevent the scaling trend in semiconductor industry, this technology brings a possibility to postpone the end of scaling trend, and pave a way for extensive application in industry.

A new method for fabrication of MOS capacitors metal gate has been developed, and lift-off process has been replaced by wet etching process. This method provides better contact between dielectric layer and metal gate, meanwhile much easier operation.

KEYWORDS: Gate Leakage Current, Silicon Oxide, Lateral Heating Process, Silicon Structure Change, Wet Etching

Lei Han

June 2, 2012

IMPROVEMENT OF SILICON OXIDE QUALITY USING HEAT TREATMENT

By

Lei Han

Dr. Zhi Chen

Director of Thesis

Dr. Zhi Chen

Director of Graduate Studies

June 2, 2012

ACKNOWLEDGMENTS

I would like to thank my academic advisor, Dr Zhi David Chen, for the opportunity he gave me to pursue my degree in the field of semiconductor devices, and all the guidance and help I've received from him all through these years. This thesis would be impossible without his extensive knowledge and innovative ideas in this field.

Special thanks should be accorded to Dr Chuck May and Brian Wajdyk for providing technical assistance at the Center for Nanoscale Science and Technology at University of Kentucky, and for helping me solving technical problems in my fabrication process.

I would also like to thank Dr. Todd Hastings, Dr. Vijay Singh, and Dr. Fuqian Yang, for serving as committee members, and for the insightful guidance I've received from them.

Thanks to my labmate, Yichun Wang, for the time and effort she spent on my fabrication training process. I would also like to thank all my group members, Dr. Youngsik Song, Dr. Chi Lu, Dr. Shibin Li, Dr. Ibrahim Yucedag, Jun Fang, Chenglin Yi, Mengmei Liu, Bojie Chen, Riasad Badhan.

Last but not least, I would like to express my deepest gratitude to my parents, for the endless love and support I have always been with since I was born.

TABLE OF CONTENTS

ACKNOWLEDGMENTS	iii
LIST OF TABLES	v
LIST OF FIGURES	vi
Chapter 1 Introduction	1
1.1 History of Device Scaling in Integrated Circuits	1
1.2 The Benefits of Device Scaling	3
1.3 Scaling of the Gate Dielectrics.....	5
1.4 Moore’s Law Is Approaching an Limitation.....	7
1.5 The Novel Phenomenon of Gate Dielectric Leakage Current Reduction	9
1.5.1 Theoretical background: Hydrogen/Deuterium isotope effect	9
1.5.2 Phonon energy coupling enhancement effect.....	11
1.6 Motivation.....	13
Chapter 2 MOS Capacitors Fabrication.....	18
2.1 RCA Clean	18
2.2 Thermal Growth of Silicon Oxide	19
2.3 Introduction and Improvement of Heat Treatment Equipment.....	21
2.4 Lift-off Process for Patterning of MOS Capacitors Gates	22
2.5 Back-side contact and post metallization annealing	24
2.6 Current-Voltage, Capacitance-Voltage characteristics measurement.....	24
Chapter 3 Wet Etch Process for Patterning of MOS Capacitors Gates	28
Chapter 4 Rapid Thermal Process with Moisture	39
Chapter 5 Lateral Heating Process Experiments and Results.....	44
5.1 Background	44
5.2 Effect of Direct Hanging and Heat Transportation.....	45
5.3 Effect of Sandwich Structure	53
Chapter 6 Conclusion and Future Work	59
6.1 Conclusion	59
6.2 Future Work	59
Reference... ..	61
Vita.....	65

LIST OF TABLES

Table 1.1: Performance parameters improvement by constant-field scaling, α is the scaling factor for dimensions ^{[9][10]}	5
Table 3.1: Thin and thick silicon oxide thickness before and after 6 minutes etching. The etchant is composed by 150ml DI water and 1g FeCl ₃ . Point 1 and 2 represent different locations on the same sample. The spectroscopic ellipsometry measurement error is less than 0.05 Å.	31

LIST OF FIGURES

Figure 1.1. Plot of CPU transistor counts against dates of introduction. Note the logarithmic scale; the fitted line corresponds to exponential growth, with transistor count doubling every two years.	15
Figure 1.2. Direct tunneling band diagram for ultra thin SiO ₂	16
Figure 1.3. FTIR spectroscopy of the phonon energy coupling enhancement (PECE) effect between the Si-O rocking mode and the Si-Si TO phonon mode before and after RTP and deuterium annealing. Tox=230Å. RTP is carried out in N ₂ at 1050°C for 4 minutes, deuterium anneal is carried out in N ₂ :D ₂ =10:1 at 450°C for 30 minutes after back side metallization ^[38]	17
Figure 2.1. Improved RTP gas system. O ₂ analyzer and dew point sensor are applied to control the O ₂ concentration and the humidity.	25
Figure 2.2. The schematic of the photolithography and lift-off process.....	26
Figure 2.3. The SEM image of the bilayer resist undercut structure.	27
Figure 3.1. Undercut of Ni pattern after FeCl ₃ etching. Photoresist was hard baked after photolithography.....	33
Figure 3.2. Undercut of Ni pattern after FeCl ₃ etching. Photoresist was not hard baked after photolithography.....	34
Figure 3.3. Severe damaged Ni gate by undercut in FeCl ₃ solution etching process.	35
Figure 3.4. Peel off of Ni sheets after diluted FeCl ₃ solution etching and ultrasonic.....	36
Figure 3.5. MOS capacitors gates achieved by wet etching process.	37
Figure 3.6. The schematic of the wet etch process. Etchant 1: 100ml DI water with 40ml HCl. Etchant 2: 150ml DI water with 1g FeCl ₃	38
Figure 4.1. Gas route to test moisture effect on heat treatment.	41
Figure 4.2. Capacitance density-voltage characteristics of n-type MOS capacitors before and after rapid thermal process with moisture exists, flatband voltages and EOTs extracted from the characteristics are marked.	42
Figure 4.3. Current density-voltage characteristics of n-type MOS capacitors before and after rapid thermal process with moisture exists.....	43
Figure 5.1. Special condition when obvious gate leakage current reduction could be available. After several times' RTP, the 4'' Si substrate became convex, and the good results are available in the sample's hanging edges.....	44
Figure 5.2. The schematic of Si step structure etching by TMAH.	49

Figure 5.3. Modification of the existing Modular Process Technology Corp. model RTP-600S system. Direct hanging and large lateral heat flow could be easily achieved with this structure.	50
Figure 5.4. Capacitance density-voltage characteristics of n-type MOS capacitors before and after lateral heating process with a substrate step structure, flatband voltages and EOTs extracted from the characteristics are marked.	51
Figure 5.5. Current density-voltage characteristics of n-type MOS capacitors before and after lateral heating process with a substrate step structure, gate leakage current densities at $V=V_{FB}+1$ are marked.	52
Figure 5.6. The top view (above) and the side view (bottom) of the RTP sandwich structure. MOS capacitors gate leakage current great reduction is observed in the hanging edge region.	56
Figure 5.7. Capacitance density-voltage characteristics of the n-type MOS capacitors before and after lateral heating process, flatband voltages and EOTs extracted from the characteristics are marked.	57
Figure 5.8. Current density-voltage characteristics of the same MOS capacitors. There is 4 to5-order-of-magnitude gate leakage current reduction after the lateral heating process.	58

Chapter 1 Introduction

1.1 History of Device Scaling in Integrated Circuits

Before the invention of semiconductor devices, vacuum tubes and relays were the dominant circuit functional devices. In the summer of 1945, Kelly, the president of Bell Laboratories at that time, built a research group. The purpose of that research group was to explore semiconductor materials, and create solid-state devices. These devices had the potential of replacing vacuum tubes and relays in circuits^[1]. This is the beginning of the development of semiconductor devices, and the effect of semiconductor devices has influenced every aspect of human's life during the past decades until nowadays. Five years after the establishment of Kelly's group, in 1950, transistor was invented^[2], which is mainly attributed to W. Shockley, J. Bardeen, and W. Brattain. In 1960s, the metal-oxide-semiconductor field-effect-transistor (MOSFET) was invented, followed by a flourishing integrated circuit era^[3]. The complementary metal-oxide-semiconductor (CMOS) technology has provided a basic element for very-large-scaled integrated circuit (VLSI), without which the modern computer science essential to almost every aspect of the society would be impossible.

Originally in 1965^[4], G. E. Moore, co-founder of Intel Corporation, brought up the *Moore's Law* for the first time, which later became one of the basic principles in integrated circuits industry. 10 years later, the *Moore's Law* was modified into the most well-known statement^[5]: *the number of transistors that can be placed inexpensively on an integrated circuit will be doubled approximately every two years*. This principle is clearly shown in Figure 1.1^[6]. During the past decades, the *Moore's Law* has always been

successful in elucidating and predicting the integrated circuits industry development path.

One of the key parameters that is applied to illustrate the semiconductor manufacture processes is the average half-pitch (i.e., half the distance between identical features in an array) of a memory cell. *The International Technology Roadmap for Semiconductors (ITRS)* named these technology nodes and used them as the milestones in the semiconductor manufacture developing trend, which are summarized as follow: 10 μm process in around 1971; 3 μm process in around 1975; 1.5 μm process in around 1982; 1 μm process in around 1985; 800 nm process in around 1989; 600 nm process in around 1994; 350 nm process in around 1995; 250 nm process in around 1998; 180 nm process in around 1999; 130 nm process in around 2000; 90 nm process in around 2002; 65 nm process in around 2006; 45 nm process in around 2008; 32 nm process in around 2010. The *ITRS* also predicted the 22 nm process approximately in 2011, 16 nm process approximately in 2013, and 11 nm process approximately in 2015^[7].

The success of integrated circuits industry with early work could be largely attributed to the success of silicon dioxide (SiO_2) as the gate dielectric for MOSFET. The properties that make SiO_2 an outstanding candidate for gate dielectric include high resistivity, excellent dielectric strength, high melting point, a large band gap and low defect density at the Si/ SiO_2 interface. Furthermore, SiO_2 could be easily grown on Si substrate at a low cost, which explains why Si has dominated the semiconductor industry for decades among other semiconductor materials such as Ge, GaAs, InP etc.

1.2 The Benefits of Device Scaling

One of the amazing things about the development of semiconductor devices is that, the MOSFET design today is not fundamentally different from the MOSFET design decades before, the performance improvement during the period is mainly brought about by “scaling”, which was discovered in 1972 by Bob Dennard of IBM^[8]. Simply speaking, scaling means the active dimensions of the integrated circuits components have been keeping decreasing. It is mainly the scaling process that provides the performance gain of 30% per generation.

The most obvious benefit of continuous scaling is higher packing density. As the MOS components become smaller, less chip area is needed for the same number of components, or more components could be integrated into the same chip area. The electronic products could then become smaller, more portable with various functions. A good example for this point is the increasing laptop memory. Additionally, in modern semiconductor technology, electronic devices on chips are fabricated using integrated methods, more components on the same chip means higher production efficiency.

Scaling reduces the RC delay of MOSFETs, providing faster devices with higher operation frequency. The main physical dimensions of transistors scaled are the channel length, channel width, and the gate oxide thickness. In this way, the transistor channel resistance, which is defined as

$$R = \rho L / A \quad (1.1)$$

(ρ is the material's resistivity, L is the channel length, A is the channel cross area), would

remain unchanged, while gate capacitance, which is defined as

$$C_{ox} = \frac{\epsilon_0 \epsilon_s}{t_{ox}} A \quad (1.2)$$

(ϵ_0 is the vacuum dielectric constant (8.85×10^{-14} F/cm), ϵ_s is the relative dielectric constant (3.9 for SiO₂), t_{ox} is the gate oxide physical thickness, and A is the area of the gate capacitor), would be cut by the scaling factor α . The time constant of a RC circuit is defined as $\tau = R \times C$, hence, the RC delay of the MOSFETs scales with the same scaling factor α . The operation frequency increases as the circuit delay decreases, as a result, the operation frequency becomes α times of the original value.

The I_{sat} of MOSFETs increases with the MOSFET scaling, which is a desirable property in high performance MOSFETs. I_{sat} is the source-drain current of MOSFETs when working in saturation region, that is the “on” mode of MOSFETs, and it acts as the driving current for the follow-up circuits. Thus, higher $I_{D,sat}$ enables higher speed of the whole integrated circuits. $I_{D,sat}$ could be written as^[9]:

$$I_{D,sat} = \frac{W}{L} \mu C_{ox} \frac{(V_G - V_T)^2}{2} \quad (1.3)$$

where W and L are the width and length of the MOSFET channel, respectively, μ is the charge carrier effective mobility, C_{ox} is the gate oxide dielectric capacitance density

($C_{ox} = \frac{\epsilon_0 \epsilon_s}{t_{ox}}$), V_G and V_T are gate voltage and threshold voltage, respectively. While W

and L are scaled by the same scaling factor α , resulting no effect on $I_{D,sat}$, the scaled t_{ox}

would result higher C_{ox} , bringing higher $I_{D,sat}$.

1.3 Scaling of the Gate Dielectrics

Many kinds of scaling concepts and technologies exist, one of them is named “constant-field scaling”. This concept proposes a scaling factor α , all of the MOSFET physical dimensions are reduced by α , the body doping concentration is increased by α , and the voltage is also reduced by the same α . In this situation, the depletion region of the MOSFETs would be scaled with the same ratio. The basic working principle is that if a constant electric field is maintained while shrinking a MOSFET, all other performance parameters would be improved, which is illustrated in table 1.1^{[10][11]}.

Table 1.1: Performance parameters improvement by constant-field scaling, α is the scaling factor for dimensions^{[10][11]}.

Parameter	Constant-field scaling
Physical dimensions	$1/\alpha$
Body doping concentration	α
Voltage	$1/\alpha$
Circuit density	$1/\alpha^2$
Capacitance per circuit	$1/\alpha$
Circuit speed	α
Circuit power	$1/\alpha^2$
Power density	1
Power-delay product	$1/\alpha^3$

Based on the principle demonstrated above, all of the MOSFET physical dimensions

should be scaled together. Plus, in order to maintain a good control of short-channel effect, the gate oxide thickness of MOSFETs should be scaled nearly in proportion to the channel length^[5]. For decades, the Intel gate oxides have been following the principle: $t_{ox}=L/45$ ^[12]. In a long period, the continuous scaling of SiO₂ had been successful until the channel length L reached 7nm, and the physical thickness of gate oxides reached under 2nm, when the gate leakage current became unacceptable^[13]. For SiO₂ gate dielectric thinner than 3 nm, the gate leakage current mechanism is mainly quantum-mechanical tunneling, especially direct tunneling^[14]. The direct tunneling band diagram is shown in Figure 1.2^[15]. It has also been reported that, in this physical thickness region, the gate leakage current magnitude will be increased by an order for each 0.2 nm decrease of the gate dielectric thickness^[16].

Based on the analysis above, a inference was made that in order to keep continuous improvement of the MOSFETs' performance, a material which is physically thick, that could be able to keep electrons from tunneling through, and electrically thin, that could be able to match the channel length scaling, was desirable. Dielectric materials with high dielectric constants (high-k) was applied to meet all the requirements, and they are becoming the dominant dielectric materials in semiconductor field. The electrical thickness of the high-k materials is decided by the "Equivalent Oxide Thickness" (EOT), which indicates how thick a SiO₂ film should be to produce the same effect as the high-k material film.

$$EOT = \frac{\epsilon_{oxide}}{\epsilon_k} t_k \quad (1.4)$$

where ϵ_{oxide} is the relative dielectric constant of SiO₂ (3.9), ϵ_k is the relative dielectric

constant of the high-k gate dielectric material, and t_k is the physical thickness of the high-k gate dielectric material. A variety of materials exist with higher k value than SiO₂, ranging from Si₃N₄ with a k value of 7, to Pb-La-Ti (PLT) with a k value of 1,400. However, a high-k dielectric material being able to substitute SiO₂ should meet certain requirements, in a systematic consideration include permittivity, band gap, band alignment to silicon, thermodynamic stability, film morphology, interface quality, compatibility with the materials used in CMOS devices processing, process compatibility, and reliability^[17].

The up-to-date channel length scaling beyond the 22 nm node requires gate dielectrics EOT < 6 Å to suppress short-channel effects^[18]. Highly scaled high-k based gate dielectrics with EOTs of 5-6 Å in nMOSFET devices have been reported^{[18][19]}. Recently, a record-setting Hf-based high-k gate dielectrics with EOT of 4.2 Å has been achieved with a “remote interfacial layer scavenging process”^[20].

1.4 Moore’s Law Is Approaching an Limitation

Questions about the end of scaling have always existed during the scaling process, although all the limitation predictions raised before have been proved to be failures. One of such predictions was the “lithography barrier,” which predicted that since photolithography process was applied in fabrication, people cannot make spatial resolution smaller than the light wavelength (157 nm for a KrCl Excimer laser)^{[11][21][22]}. Another such predictions was the “oxide scaling barrier,” which claimed that since the gate leakage current becomes unacceptable when the gate oxide thickness is below 3 nm,

this is the final barrier for scaling^{[11][23][24]}.

However, the continuous scaling process cannot last forever, an ultimate limitation will come sooner or later. MOSFETs can only be effective when they can maintain switch functions^[25], which means MOSFETs should be able to provide a sufficient drive current during the “on” state, and a low enough leakage current during the “off” state. Satisfactory drive current is available with MOSFETs’ scaling as illustrated before, the main challenge is to maintain low “off” state leakage current, which is mainly consisted of thermionic emission above the channel potential barrier, band-to-band tunneling between the body and drain p-n junction, and quantum mechanical tunneling directly between the source and drain^[25]. Additionally, the gate dielectrics EOT has already been scaled down to a few angstroms, which is just several atomic layers. In 2003, Intel claimed that the transistors cannot be scaled below the size achievable at 16 nm process (5 nm gate dielectrics) due to quantum tunneling, regardless of the materials used, and the scaling deadline is predicted to lay in between 2013 and 2018^[26]. On April 13rd, 2005, G. E. Moore also stated in an interview himself that the *Moore’s Law* cannot be sustained indefinitely.

In order to prolong the electronic components scaling limitation which is already above the horizon, innovative materials, techniques and device ideas are continuously desirable, among which an institution to silicon-based CMOS technique is attracting more and more research enthusiasm. The non-silicon extension of CMOS, such as III-V materials^[27] and nanotubes/nanowires based devices^{[28][29]}, as well as non-CMOS platforms, such as

molecular electronics^[30], spin-based computing^[31], and single-electron devices^[32], have been proposed. However, those exotic materials and devices have their own limitations, especially when they are aimed for large scale manufacturing. Therefore, exploring novel phenomena for improvement of silicon based MOS devices is still very important.

1.5 The Novel Phenomenon of Gate Dielectric Leakage Current Reduction

1.5.1 Theoretical background: Hydrogen/Deuterium isotope effect

Due to high electric field in the scaling MOSFETs' channel, some carriers in the channel are ionized, which obtain larger energy level than the thermal energy in equilibrium. These carriers are termed as hot carries, and they could achieve an exceedingly high velocity. Even though these hot carriers could increase the speed of MOSFETs, they could also have adverse effects on the reliability of devices, especially on the increasing of Si dangling bonds at the Si/SiO₂ interface. The Si dangling bonds are referred to as interfacial traps, and they degrade the performance of MOSFETs. Post metallization annealing in hydrogen ambient is carried out to passivate the Si dangling bonds, but the resulting Si-H bonds are not stable, which could be easily broken by energetic hot carriers in the channel.

Lyding et al. compared the passivation of the Si dangling bonds with both hydrogen and deuterium^[33], and it is proved that the Si-D bonds are more resistive to hot electron degradation than Si-H bonds. This is the hydrogen/deuterium isotope effect: Si-D bonds are

much stronger than Si-H bonds. By applying deuterium annealing, the hot electron degradation could be improved by ~50 times^{[33][34][35]}.

Van de Walle et al. explained the hydrogen/deuterium isotope effect with two competing processes^[36]: (1) the vibrational energy of bonds is accumulated through multiple vibrational excitation by energetic hot electrons in the low voltage regime. The energy of the bonds is increased to a point where the bonds are broken; (2) an opposite de-excitation process exists, where the vibrational energy of the Si-D bonds are reduced by energy coupling to the Si-Si TO phonon mode in the substrate. While there is almost no coupling between the Si-H bending mode (650 cm^{-1}) and the Si-Si TO phonon mode (463 cm^{-1}), there is strong coupling between the Si-D bending mode (460 cm^{-1}) and the Si-Si TO phonon mode. The de-excitation process is much more efficient with the Si-D bonds than the Si-H bonds, which leads to the conclusion that the Si-D bonds are more robust to hot electron degradation than the Si-H bonds.

1.5.2 Phonon energy coupling enhancement effect

Certain mismatch has been reported between the Si-D vibrational mode and the Si-Si TO phonon mode^[37], and it was also observed in the previous work of our lab^[38]. Dr. Zhi David Chen, professor in Department of Electrical and Computer Engineering, University of Kentucky, made the assumption that in the Si/SiO₂ system, if the Si-D vibrational mode could be shifted toward the Si-Si TO phonon mode, the hydrogen/deuterium isotope effect might be tremendously enhanced. Rapid Thermal Process (RTP) was used to supply thermal stress, which is supposed to introduce the atomic bonds vibrational modes shift.

By applying the RTP directly on thermally grown SiO₂, phonon energy coupling enhancement effect was found by Dr. Chen and his students^{[39][40][41][42][43]}. Fourier-Transform-Infrared (FTIR) spectroscopy is applied to prove the assumption, which is shown in figure 1.3, along with the process parameters of RTP and deuterium anneal. While there is no obvious shift of the Si-D vibrational mode and the Si-Si TO phonon mode, which means the coupling between these two modes have not been strengthened, there is large increase in the FTIR absorption intensity after RTP, the absorbance of the Si-Si TO phonon mode and the Si-O TO rocking mode are tremendously enhanced. The phonon energy coupling enhancement happens between the Si-Si TO phonon mode and the Si-O TO rocking mode, and the Si-Si TO phonon mode intensity is increased by about 50% after RTP^[38].

The electrical characteristics of devices are also achieved, which provide more experimental evidences for the phonon energy coupling enhancement effect. Large size

MOSFETs were fabricated in our lab, and large drain and gate voltages were applied to investigate the hot electron degradation. The larger the threshold voltage shift is, the more degradation is in the devices. It has been certified that after RTP and deuterium anneal, the threshold voltage shift was tremendously suppressed. The Si-D bonds become much more robust after RTP^{[40][43]}.

The gate oxide breakdown tests were carried out to test the strength of the Si-O bonds. With a SiO₂ thickness around 20 nm, the breakdown voltage could be improved by 30%-40% with the RTP samples comparing to control samples which are not subjected to RTP^[43]. The Si-O bonds become more robust after RTP.

Special p-n junction diode, with which one side of the substrate is thermally grown SiO₂, the other side of the substrate is p-n junction diode, was fabricated and tested for breakdown voltages. Comparing to the control samples whose SiO₂ layers have not went through RTP (with the breakdown voltage around 7.4 volts), the RTP samples' breakdown voltage is increased by around 0.3 volts^[44]. The Si-Si bonds become more robust after RTP.

In fact, during the process of proving the phonon energy coupling enhancement effect, the atomic bonds strength enhancement turned out to be a side effect, while a novel phenomenon became the most impressive: after RTP, the gate leakage current of the MOS capacitors has been greatly reduced^[38-44]. For thick SiO₂ (around 10 nm), 2-order-of-magnitude gate leakage current reduction has been reported; for ultrathin SiO₂ (less than

3.5 nm), 3 to 5-order-of-magnitude gate leakage current reduction has been reported.

1.6 Motivation

Although materials with high dielectric constant are the mainstream dielectric materials in semiconductor industry nowadays, silicon oxide is still unavoidable. Direct deposition of high-k dielectric layer cannot avoid gaps between dielectric layer and semiconductor substrate, and the trap charges exist in the interface, even atomic layer deposition (ALD) is applied^[45]. In order to get gate dielectric layer with high quality, the native oxide layer on the Si substrate must be removed; governed by the working principle of ALD, H-terminated Si (H/Si) substrate is necessary for thin film growth. Both of these purposes could be easily achieved by RCA cleaning and hydrofluoric acid (HF) etches. However, the H-terminated Si substrate is thoroughly hydrophobic, which results a large barrier to HfO₂ nucleation process. The ALD growth with this nucleation barrier is characterized by nonlinear growth rate and discontinuous interior structure, which serves as electric leakage path. Thus, a SiO_x interfacial layer with satisfactory properties is desired.

The underlying mechanism of the phenomenon, impressive gate leakage current reduction, is still not clear. Is it because of *phonon energy coupling enhancement (PECE)*, or some unknown material structure changes? The conditions which cause the gate leakage current reduction are crucial. Without clear understanding, it is very difficult to produce the gate leakage current reduction effect reproducibly. Because this effect can reduce the tunneling current of gate oxide, it is of great interest to use this effect to reduce the leakage current of high-k gate oxide stacks, which may further improve the properties of the

silicon MOS devices, and pave a way for extensive applications of this technology in industry.

CPU Transistor Counts 1971-2008 & Moore's Law

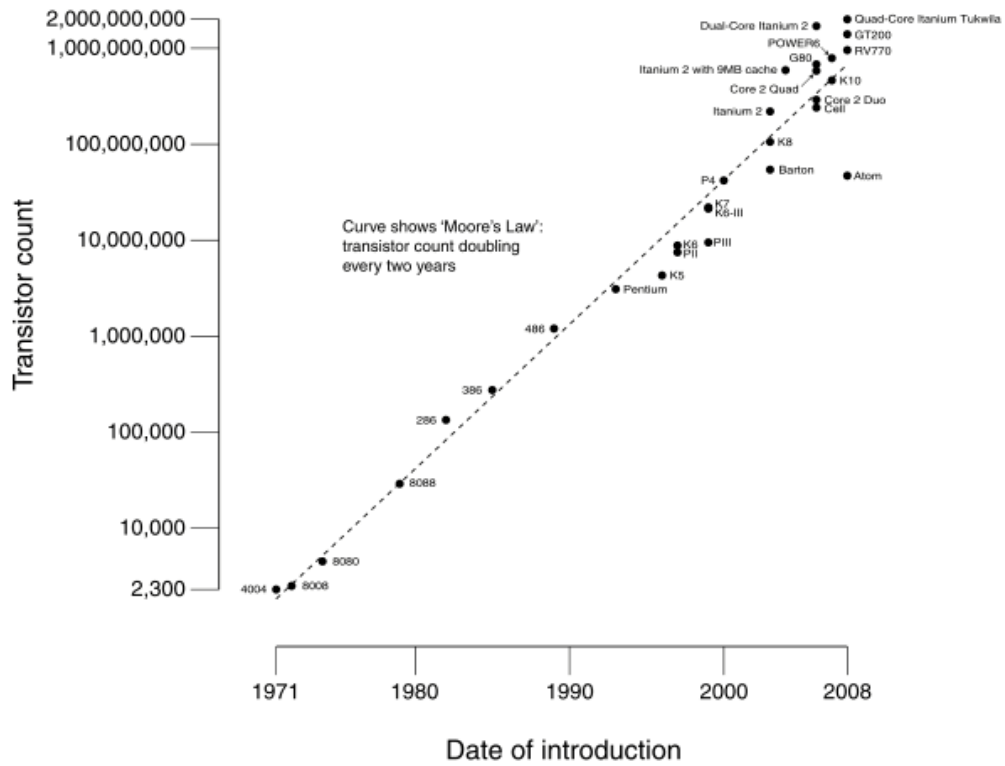


Figure 1.1. Plot of CPU transistor counts against dates of introduction. Note the logarithmic scale; the fitted line corresponds to exponential growth, with transistor count doubling every two years^[6].

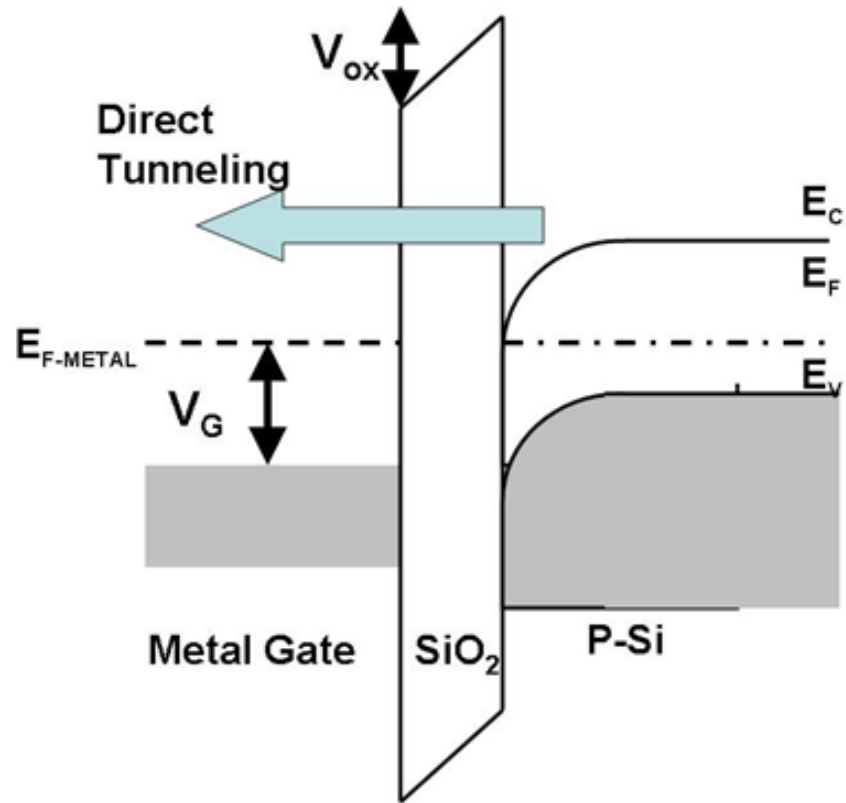


Figure 1.2. Direct tunneling band diagram for ultra thin SiO₂^[14].

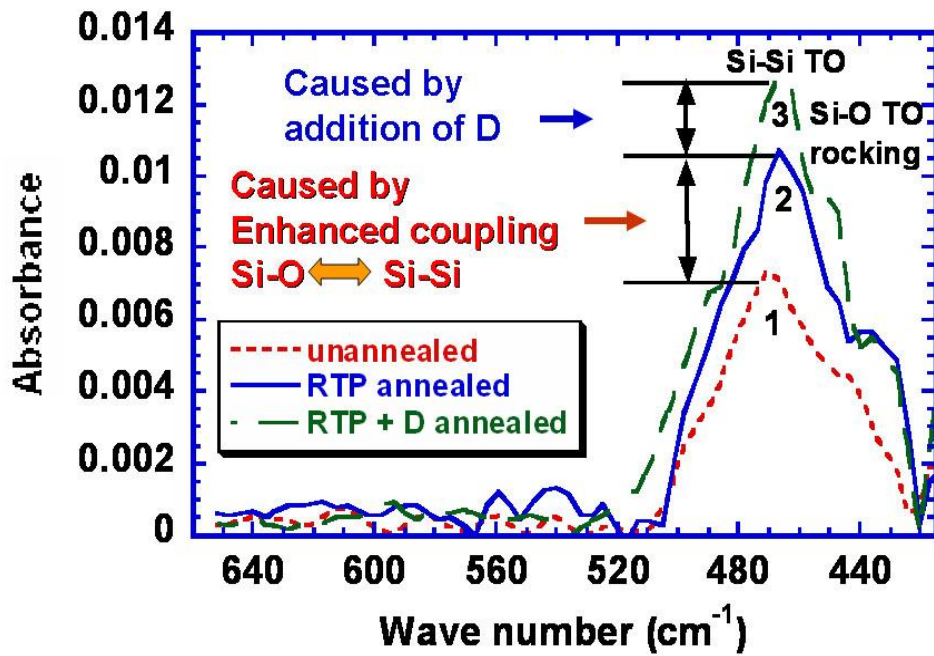


Figure 1.3. FTIR spectroscopy of the phonon energy coupling enhancement (PECE) effect between the Si-O rocking mode and the Si-Si TO phonon mode before and after RTP and deuterium annealing. $T_{ox}=230\text{\AA}$. RTP is carried out in N_2 at 1050°C for 4 minutes, deuterium anneal is carried out in $N_2:D_2=10:1$ at 450°C for 30 minutes after back side metallization^[38].

Chapter 2 MOS Capacitors Fabrication

In order to characterize silicon oxide material properties after heat treatment, simple MOS capacitors with SiO₂ as gate dielectric layer are fabricated, and current-voltage (I-V), capacitance-voltage (C-V) curves are tested. Key parameters which reflect properties of MOS capacitors, such as flatband voltage (V_{FB}) and equivalent-oxide-thickness (EOT), could be extracted from the curves.

2.1 RCA Clean

RCA cleaning is a standard set of silicon wafer cleaning steps in semiconductor manufacturing which needs to be performed before any crucial steps, especially high temperature processing steps.

RCA cleaning was firstly developed by Werner Kern in 1965, while he was working for RCA, the Radio Corporation of America^[46]. The purposes of the RCA cleaning, listed according to the cleaning steps, are to remove organic contaminants (such as dust particles, grease or silica gel) from the wafer surface; then remove any oxide layer that may have built up during the prior steps; finally remove any ionic or heavy metal contaminants^[47].

The RCA cleaning procedures are listed below:

Step 1: Removal of grease, etc.

- (1) Acetone cleaning with ultrasonic machine, 3 minutes.
- (2) Isopropyl alcohol cleaning with ultrasonic machine, 3 minutes

(3) Thoroughly rinse with DI water (deionized water).

Step 2: Removal of native oxide.

(1) Immerse in a (20:1) solution of DI water: HF for 30 seconds.

Check the sample surface is hydrophobic or hydrophilic after this step. Bare Si surface should be hydrophobic. If the surface is still hydrophilic, there is still SiO₂ residual, the sample needs to be etched for longer time.

(2) Thoroughly rinse with running DI water in 30 seconds.

This step should be finished in 30 seconds, otherwise Si oxide layer will grow again.

Step 3: RCA 1 (or SC 1), removal of organic (dust particles, grease or silica gel) / metal ionic (Cu, Ag, etc.) contamination.

(1) Immerse in a (5:1:1) solution of DI water: NH₄OH: H₂O₂ at 75-80°C for 10 minutes.

(2) Thoroughly rinse with DI water.

Step 4: Removal of chemical oxide formed during RCA 1.

(1) Immerse in a (20:1) solution of DI water: HF for 30 seconds.

(2) Thoroughly rinse with running DI water in 30 seconds.

Step 5: RCA 2 (or SC 2), removal of heavy metal contamination and alkali ions.

(1) Immerse in a (5:1:1) solution of DI water: HCl: H₂O₂ at 75-80°C for 10 minutes.

(2) Thoroughly rinse with DI water.

2.2 Thermal Growth of Silicon Oxide

In the exploration of the leakage current reduction mechanism, both ultrathin and rela-

tively thick SiO₂ have been grown to serve as the gate dielectric layer.

Various techniques are available to grow or deposit silicon oxide/dioxide films. Electrochemical anodization, plasma-enhanced chemical vapor deposition (PECVD) and sputtering are some examples. Among all the techniques, thermal oxidation growth of Si dioxide films provides the highest quality with the lowest interface trap densities. Thermal oxidation can be realized in an atmosphere containing dry oxygen gas (dry oxidation) or water vapor (wet oxidation). In our experiment, we use dry thermal oxidation to get exact control of oxidation thickness.

For single-crystal Si wafers, the Deal-Grove model describes the SiO₂ growth principle^[48]. However, very thin oxides (less than 25 nanometers) grow much faster than the model predicts. This is the situation in our experiments.

Ultrathin SiO₂ layer (around 20 Å) could be achieved by diluted O₂, the high temperature oxidation furnace is provided by *Lindberg Furnace*. Based on our experiences, at temperature 900°C, with the flow rate of N₂:O₂ equals 5:1, oxidation time ranges from 20 to 40 seconds, we can controllably get SiO₂ layer around 20 Å with high quality on the (1 0 0) Si wafer. The thickness and optical properties of the thin film could be measured with the spectroscopic ellipsometer (*J. A. Woollam Co.*, M-2000V model).

Before oxidation process, native oxide is removed by BOE etching, enabling good interface properties. Post-Oxidation-Annealing (POA) is also executed in order to reduce

fixed oxide charges.

The referred SiO₂ is just “thick” comparing to the ultrathin SiO₂, it is still considered as thin SiO₂ in the common sense, and it still follows the growth principle for thin SiO₂. Based on our experiences, at temperature 900°C, with pure O₂, after oxidation for 20 minutes, we can controllably get SiO₂ layer 90-100 Å thick with high quality on the (1 0 0) Si wafer.

2.3 Introduction and Improvement of Heat Treatment Equipment

Rapid Thermal Process (RTP) system is utilized to realize the heat treatment experiments. RTP refers to a semiconductor manufacturing process which heats silicon wafers to high temperature (up to 1200°C or greater) on a timescale of several seconds or less. During cooling, wafer temperature must be brought down relatively slowly so the wafer does not break due to thermal shock. RTP has been widely used as a standard technique in semiconductor manufacturing including rapid thermal annealing, dopant activation, thermal oxidation, metal reflow and chemical vapor deposition. The RTP system used in our experiments is from *Modular Process Technology Corp.*, model RTP-600S, in which the light radiation comes from two banks of linear tungsten-halogen lamps, acting as the energy source.

The processing gas applied in the lateral heating process is N₂ or He. Based on our experience, He provides higher cooling rate than N₂. Additionally, trace O₂ is needed in N₂ or He since without trace O₂, SiO₂ decomposes at high temperature (>1000°C)^[42]. How-

ever, O₂, plus humidity, can cause thermal oxidation of Si within high temperature, and precise control of a small amount of O₂ (200-500 ppm) and humidity is desirable to avoid unacceptable SiO₂ regrowth.

The concentration of O₂ is measured using a trace O₂ analyzer (Alpha Omega Series 3000, with a measure range of 1-10000 ppm), which can be connected both to the processing gas input pipe and the output pipe. By monitoring the O₂ concentration in these pipes, we can exactly tell the O₂ concentration in the chamber during the lateral heating process. The O₂ analyzer is followed by a dew point sensor, in order to control the humidity in the chamber during the process. The schematic of the improved RTP gas system is shown in figure 2.1.

2.4 Lift-off Process for Patterning of MOS Capacitors Gates

The MOS capacitors fabricated in our experiments are circles with diameter 100 μm. The bi-layer resist photolithography and the lift-off process have been applied to pattern the MOS capacitors gate, which have been reported in the publications of our lab before^{[49][50]}. The *ShIPLEY* 1813 and the SU-8 2001 from *Microchem* serve as the positive and negative photoresists. Since the SU-8 2001 developer (from *Microchem*) consists of 98% 1-Methoxy-2-propyl acetate (C₆H₁₂O₃), which is a solvent for the S1813, no matter whether the S1813 has went through exposure or not, an undercut structure could be formed after the development. The schematic of the photolithography and lift-off process is shown in figure 2.2, and the SEM image of the bilayer resist structure is shown in figure 2.3.

In the previous work of our lab^{[39][40][41][42]}, Al was deposited by thermal evaporation through shadow masks to form the MOS capacitor gate, in order to get rid of the photoresist. Post-metal annealing (PMA) was required to ensure low interface trap density and good ohmic contact; without PMA, an air gap exists between the Al gate and the SiO₂ dielectric, which decreases the accumulation region capacitance of the MOS capacitors. However, Al is known to diffuse through ultrathin oxides (<30Å) at PMA temperatures (~450°C), causing short-circuit of the devices.

Ni has excellent thermal stability (low/negligible diffusion through oxides at PMA temperature). However, the melting temperature of Ni is high and it could only be deposited by either e-beam evaporator or sputtering machine. Plasma in sputtering machine can damage the ultrathin oxides by energetic ion bombardment, thus, e-beam evaporator is chosen for Ni gate metallization, and a good metal gate thickness is 1000Å.

This photolithography and lift-off process for the Ni gate patterning has been working effectively with low price; however, a drawback exists that there has always been the risk of peeling off. We made the assumption that there are always organic remains after development. In order to prove this assumption, samples with prolonged development time were fabricated, and a phenomenon was observed that, while all samples show satisfactory undercut structures under microscope after photolithography, the longer the development time is, the more severe the peeling off problem shows. Thus, the development process must have left certain organic remains.

2.5 Back-side contact and post metallization annealing

The back-side contact is made by a 1000Å Al film which is also deposited by e-beam evaporator. During this process, the front-side of the sample is protected by hard baked S1813.

The post metallization annealing is executed at 450°C in forming gas (N₂:H₂ = 10:1) for 30 minutes at a pressure of 1 atmosphere.

2.6 Current-Voltage, Capacitance-Voltage characteristics measurement

The capacitance-voltage characteristic is measured using a HP 4284A precision LCR meter at 100 KHz, since the frequency dispersion is negligible, and the equipment is able to provide measuring frequencies from 1 K to 1 MHz. The current-voltage characteristic is measured using an Agilent 4155B semiconductor parameter analyzer.

The EOT and the flatband voltage of the capacitors are extracted from the C-V characteristic via UC Berkeley Quantum-Mechanical Simulator (taking quantum correction into consideration). The ideal C-V characteristic is simulated and used to fit the experimental C-V characteristic. The current density is compared at the voltage $V_G = V_{FB} + 1$.

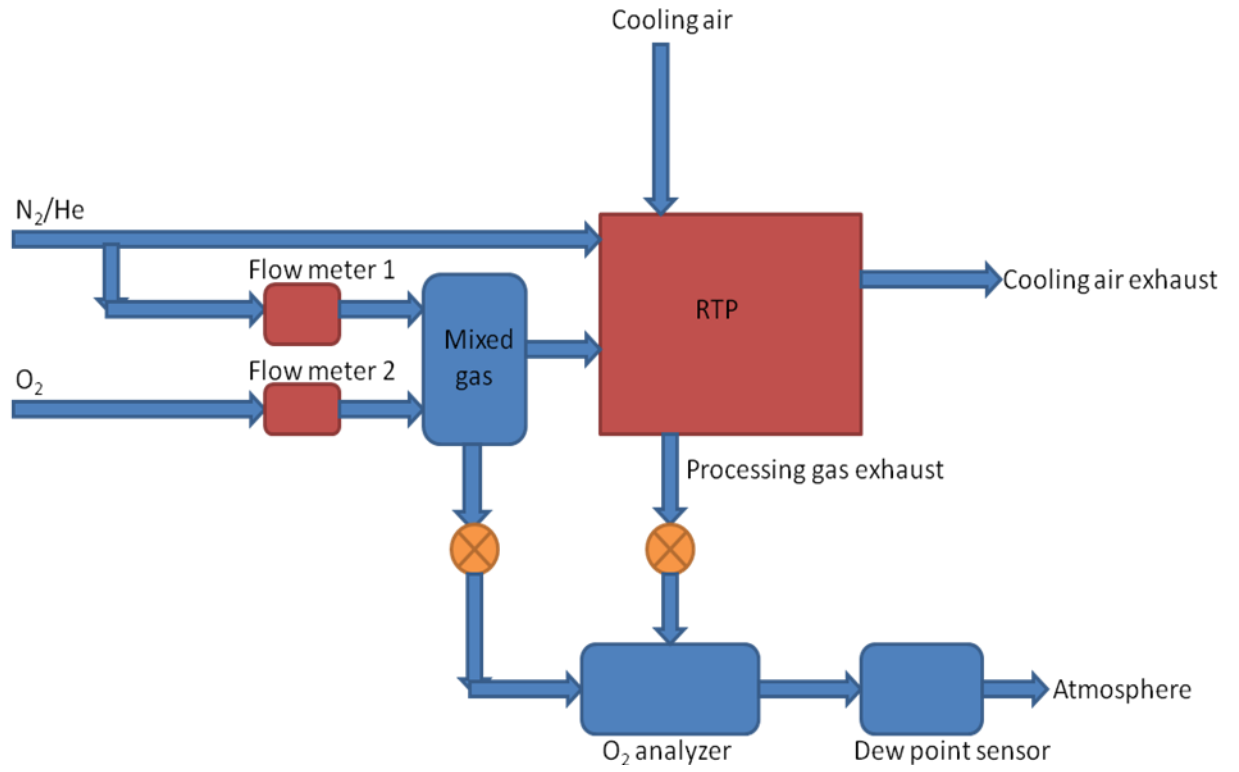


Figure 2.1. Improved RTP gas system. O₂ analyzer and dew point sensor are applied to control the O₂ concentration and the humidity.

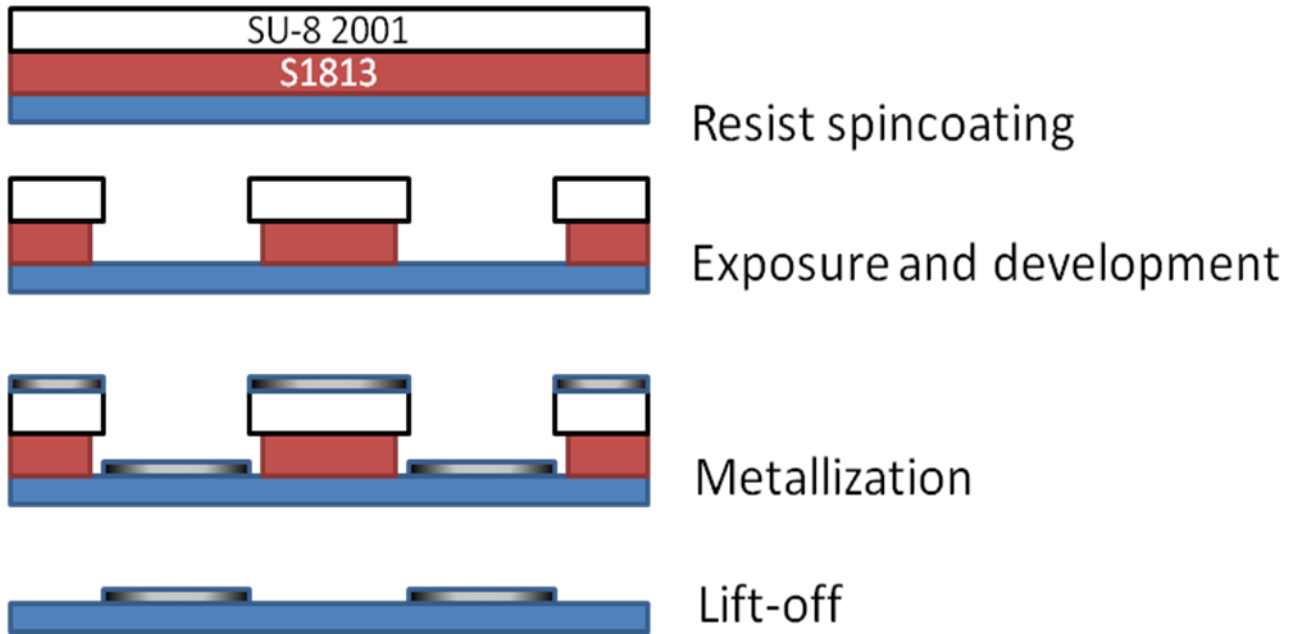


Figure 2.2. The schematic of the photolithography and lift-off process.

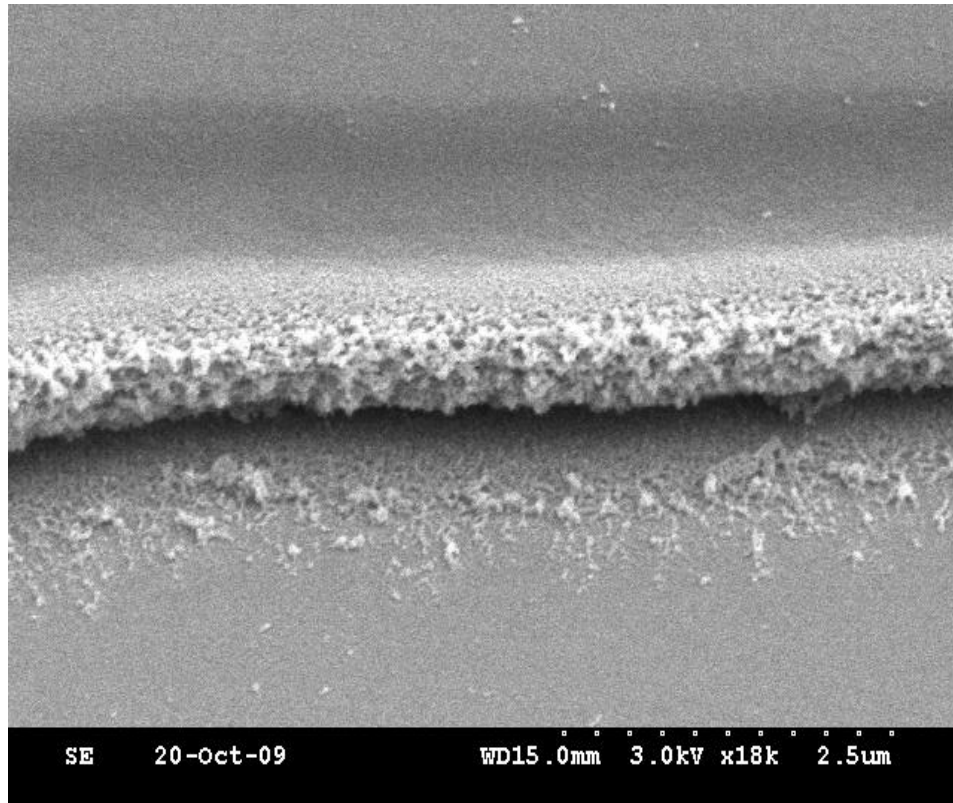


Figure 2.3. The SEM image of the bilayer resist undercut structure.

Chapter 3 Wet Etch Process for Patterning of MOS Capacitors Gates

The drawbacks of lift-off process for MOS capacitors patterning is obvious: peeling off problem requires that the photolithography parameters must be precisely controlled, otherwise, even a tiny experiment condition change can cause severe problem. This introduces unnecessary difficulty into the experiment operation. Plus, the peeling off problem shows the contact between metal gate and dielectric material is not ideal, organic remains exist between metal gate and dielectric material, which could affect electrical properties of MOS capacitors.

Wet etching is another way to pattern MOS capacitors gate. In this situation, metal is directly deposited onto dielectric layer without touching any organic solutions, so there would be no gap between metal gate and dielectric material, and the contact is guaranteed. Several solutions have been reported as etchant for Ni, such as HCl: HNO₃=5:1 solution, HF: HNO₃=1:1 solution, ect^{[51][52]}. However, a solution including acid could cause damage to silicon oxide, which is unacceptable. FeCl₃ solution is a satisfactory candidate for our purpose, since it has the ability of etching Ni, while does not attack silicon oxide.

I started with 30% FeCl₃ solution to work on our 1000Å Ni. S1813 was used to do photolithography. After exposure and development, the pattern areas are protected with photoresist. Then sample are immersed into FeCl₃ solution. The etching rate was so high that all the Ni was etched away very fast. I started to dilute the FeCl₃ solution. Although etching rate became lower, it was impossible to control the etching, severe undercut always happened before Ni without photoresist protection is gone. After photoresist spincoating,

a tiny gap could exist between photoresist and Ni, I assumed that FeCl_3 solution could flow into this gap and make a direct contact with Ni, which is supposed to be under protection. This gap could be fixed by hard bake of photoresist. Then hard bake was applied on the sample after development (140°C for 3 minutes). However, this does not improve this situation at all. The undercut problem is as serious with the hard baked sample as the non-hard baked sample. If I etched samples until the un-protected part Ni is almost gone, there is always undercut on the Ni pattern edge. This proves the gap between photoresist and Ni is not the problem. Both the samples with and without photoresist hard bake are shown in figure 3.1 and 3.2. After removing photoresist by Remover PG, we could see that the patterns are severely damaged, which is shown in figure 3.3.

Since the undercut problem was severe, either the etching rate of Ni by FeCl_3 solution must be still too high, or the etching time must be too long. Since the etching time was already under 1 minute, the etching rate must be unacceptable. Does further dilution of FeCl_3 help? I immersed sample into further diluted FeCl_3 sample, and it started to be very difficult to get rid of Ni, even on the parts without photoresist protection. Then I used ultrasonic to help, and Ni started to peel off with huge sheets, which does not follow the photolithography pattern at all. This is shown in figure 3.4. Thus, diluted FeCl_3 solution cannot provide satisfactory patterns.

Return to the situation with undercut. It is obvious that the Ni etching rate must be too high, otherwise there cannot be undercut within 1 minute. But why there is always Ni residuals on the parts without photoresist protection? Why Ni could not be etched uniform-

ly; some areas totally gone, while other areas seem like totally untouched? We assume this is because Ni is very easy to be oxidized, the top layer Ni directly contacts with oxygen in the atmosphere, so a thin layer of Ni_xO_y exists above the metal layer after evaporation. This thin layer of Ni_xO_y is not uniform among the whole sample surface, on the areas where this layer exists, the FeCl_3 solution are blocked from touching Ni underneath; on the other areas without this block, Ni is etched away fast. In order to prove this assumption and get uniform etching among the whole sample, it is desirable to get rid of this Ni_xO_y layer. Hydrochloric acid (HCl) solution provides an easy way to etch away Ni_xO_y . Since this layer is thin, only low concentration and short time is needed. Based on our experiment, 100ml DI water with 40ml HCl is able to etch away all Ni_xO_y in 1 minute. This solution has a really low etching rate on Ni, so over-etching does not need to be worried.

With HCl solution etching added before FeCl_3 solution etching, satisfactory patterns are achieved. The Ni under photoresist could maintain almost untouched, while the other Ni are all gone. This is shown in figure 3.5, and the FeCl_3 solution concentration which provides best result is 150ml DI water with 1g FeCl_3 . Higher concentration can result in a little undercut.

Damage of silicon oxide is not acceptable, so experiment was done to prove that this etchant does not affect silicon oxide. Both thin and thick silicon oxide are tested. Growth of thin and thick silicon oxide are demonstrated in 2.2. The original silicon oxide thicknesses are measured by spectroscopic ellipsometry (SP), and then samples are immersed

into etchant, which is consisted by 150ml DI water and 1g FeCl₃. After 6 minutes etching, samples are taken out, and the thicknesses are measured again by SP. The thicknesses before and after etching are compared, and the results are listed in table 3.1.

Table 3.1: Thin and thick silicon oxide thickness before and after 6 minutes etching. The etchant is composed by 150ml DI water and 1g FeCl₃. Point 1 and 2 represent different locations on the same sample. The spectroscopic ellipsometry measurement error is less than 0.05Å.

	Thickness before etching	Thickness after etching
Sample 1 point 1	27.55 ±0.05 Å	26.56 ±0.05 Å
Sample 1 point 2	27.81 ±0.05 Å	27.07 ±0.05 Å
Sample 2 point 1	102.18 ±0.05 Å	101.26 ±0.05 Å
Sample 2 point 2	103.59 ±0.05 Å	103.11 ±0.05 Å

From the results listed in the table, it is obvious that after direct contact etching, there is only tiny decrease of silicon oxide thickness (<1Å). Considering the SP measurement error, the decrease is possible to be caused by SP measurement error. In our real MOS capacitors gate patterning process, the maximum time used to etch 1000Å Ni is 2 and half minutes, during which the dielectric layers are protected by Ni and photoresist, so the 6 minutes direct contact etching test can prove that the FeCl₃ etchant introduces no harm to silicon oxide dielectric layers.

With Ni_xO_y etching taken into consideration, the whole wet etching procedure for patterning of MOS capacitors gate is achieved, and it is summarized as follow: (1) 1000Å Ni

is deposited directly onto silicon oxide dielectric layer. (2) Photolithography on Ni, while the MOS capacitors gates areas are protected by photoresist. (3) Immerse samples into etchant 1, which is composed of 100ml DI water and 40ml HCl, this is to get rid of Ni_xO_y on top. (4) Immerse samples into etchant 2, which is composed of 150ml DI water and 1g FeCl_3 , this is to etch unwanted Ni parts. (5) Immerse samples into Remover PG at 100°C for 10 minutes, this is to get rid of photoresist. The schematic of the whole wet etching procedure is shown in figure 3.6. With this procedure, satisfactory patterning of MOS capacitors gates could be easily got.

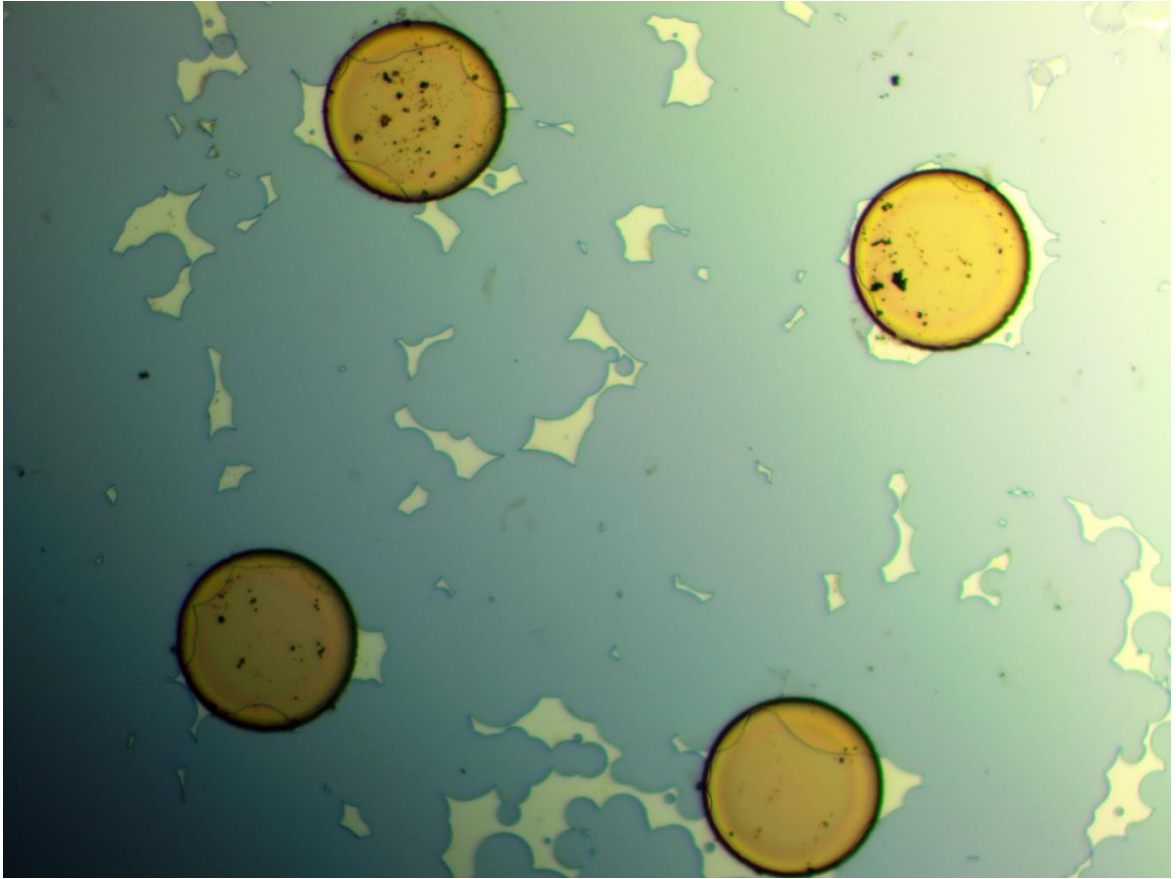


Figure 3.1. Undercut of Ni pattern after FeCl_3 etching. Photoresist was hard baked after photolithography.

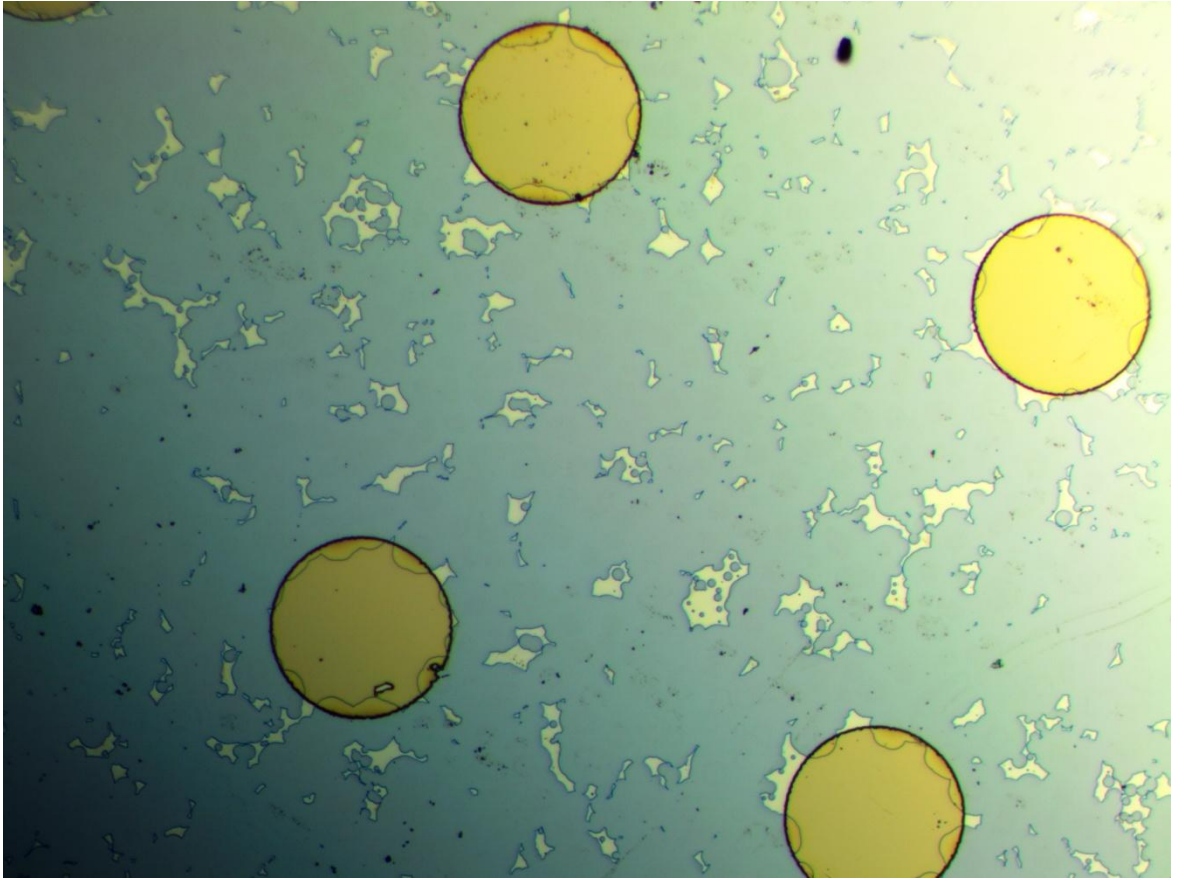


Figure 3.2. Undercut of Ni pattern after FeCl_3 etching. Photoresist was not hard baked after photolithography.

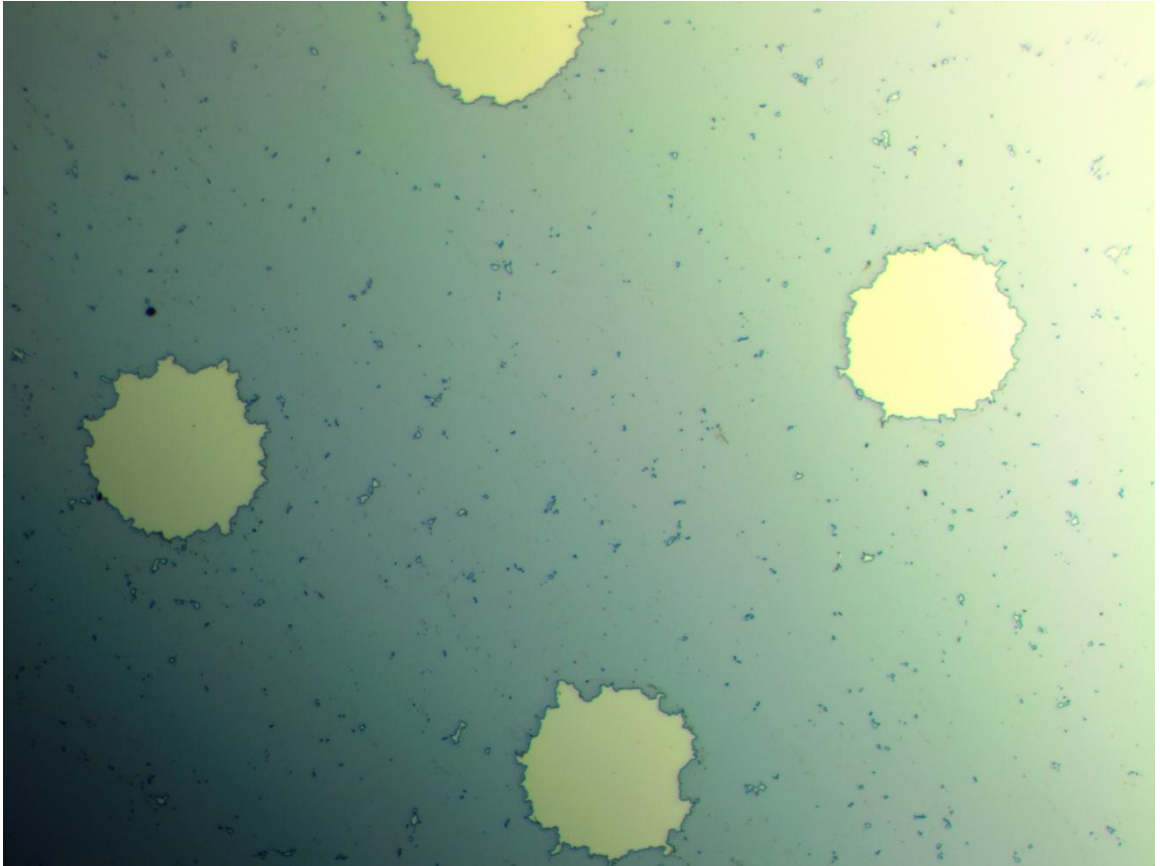


Figure 3.3. Severe damaged Ni gate by undercut in FeCl_3 solution etching process.

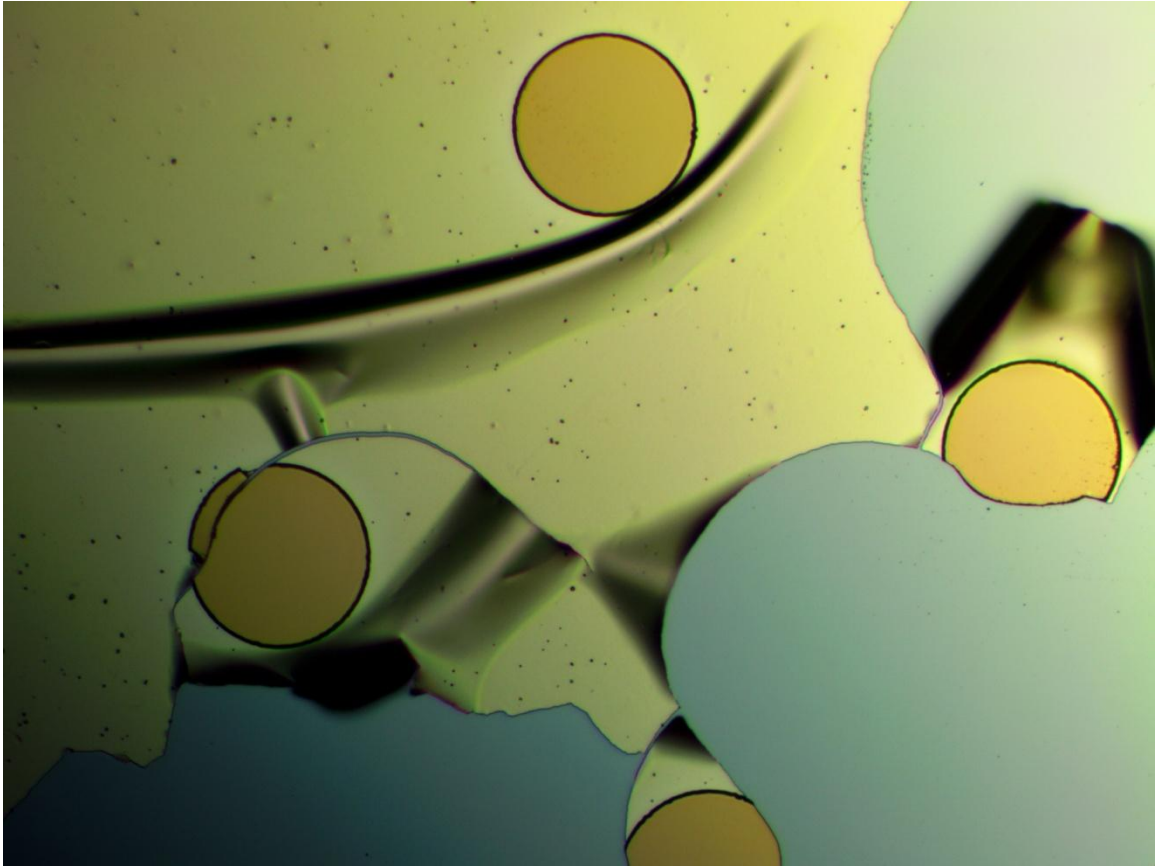


Figure 3.4. Peel off of Ni sheets after diluted FeCl_3 solution etching and ultrasonic.



Figure 3.5. MOS capacitors gates achieved by wet etching process.

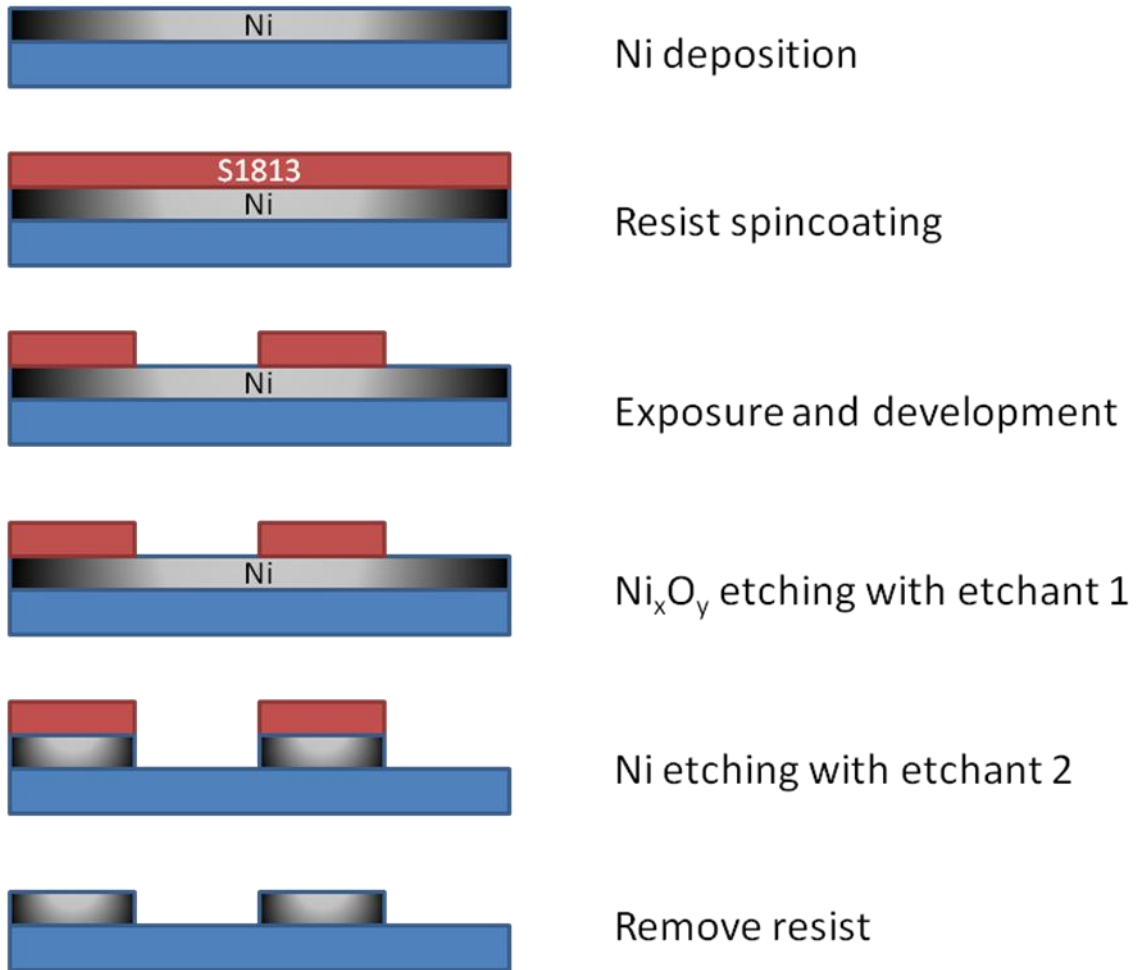


Figure 3.6. The schematic of the wet etch process. Etchant 1: 100ml DI water with 40ml HCl. Etchant 2: 150ml DI water with 1g FeCl_3 .

Chapter 4 Rapid Thermal Process with Moisture

It has been reported that a SiO_2 transition layer exists between Si and SiO_2 in thermally grown SiO_2 film. Since SiO_2 has a large volume expansion upon oxidation, Si at the interface is under a tension and strained^[53]. This phenomenon looks similar to our experiment situation. The SiO_2 stated in the original paper was grown by wet oxidation. In order to test the effect of moisture on the gate leakage current reduction, we re-built the gas route of RTP system. This route is shown in figure 4.1.

Helium is used as processing gas, and trace O_2 is replaced by moisture. This is realized by flowing N_2 through a flask with water inside. Pure He and He with moisture combine together before entering into a humidity sensor, which is utilized to control the relative humidity level. The mixture gas is then directed to RTP chamber, and trace O_2 analyzer is still applied to control the O_2 concentration in the mixture gas.

A 4 inch Si wafer was used as substrate, and a quarter of 2 inch n-type Si wafer with thermally grown ultrathin SiO_2 is put onto this substrate. The temperature inside the RTP chamber was increased with a rate of $10\text{ }^\circ\text{C}/\text{second}$, until it reached 1000°C , then hold for 60 seconds. 1000°C was chosen since it has been reported that in temperature higher than 1000°C , lattice distortion in Si substrate would reduce because of viscous flow of SiO_2 ^[53]. The relative humidity level was 50.1%.

After heat treatment, MOS capacitors were fabricated and tested, the capacitance density-voltage (C-V) and current density-voltage (I-V) properties are shown in figure 4.2 and

4.3. The flatband voltages (V_{FB}) are consistent with all the control and RTP samples. Equivalent oxide thickness (EOT) of control sample is less than 20\AA , and RTP samples is more than 24\AA , which means after RTP, the ultrathin SiO_2 got around 5\AA regrowth.

From figure 4.3, it is obvious that after RTP, there is 3 orders of magnitude gate leakage current density reduction. The 5\AA regrowth of SiO_2 dielectric layer corresponds to 2.5 order of magnitude reduction^[16], and this should be substrated from the 3 orders. Taking the SiO_2 thickness increase into consideration, we could conclude that RTP is responsible for 0.5 order of magnitude gate leakage current density reduction. This phenomenon is uniform among all the devices in this sample, which is an effective way to provide MOS devices with a little higher quality. However, 0.5 order is far less than our expected 3-5 order of magnitude gate leakage current reduction. The underlying mechanism for our tremendous improvement of MOS devices' electrical properties is not moisture.

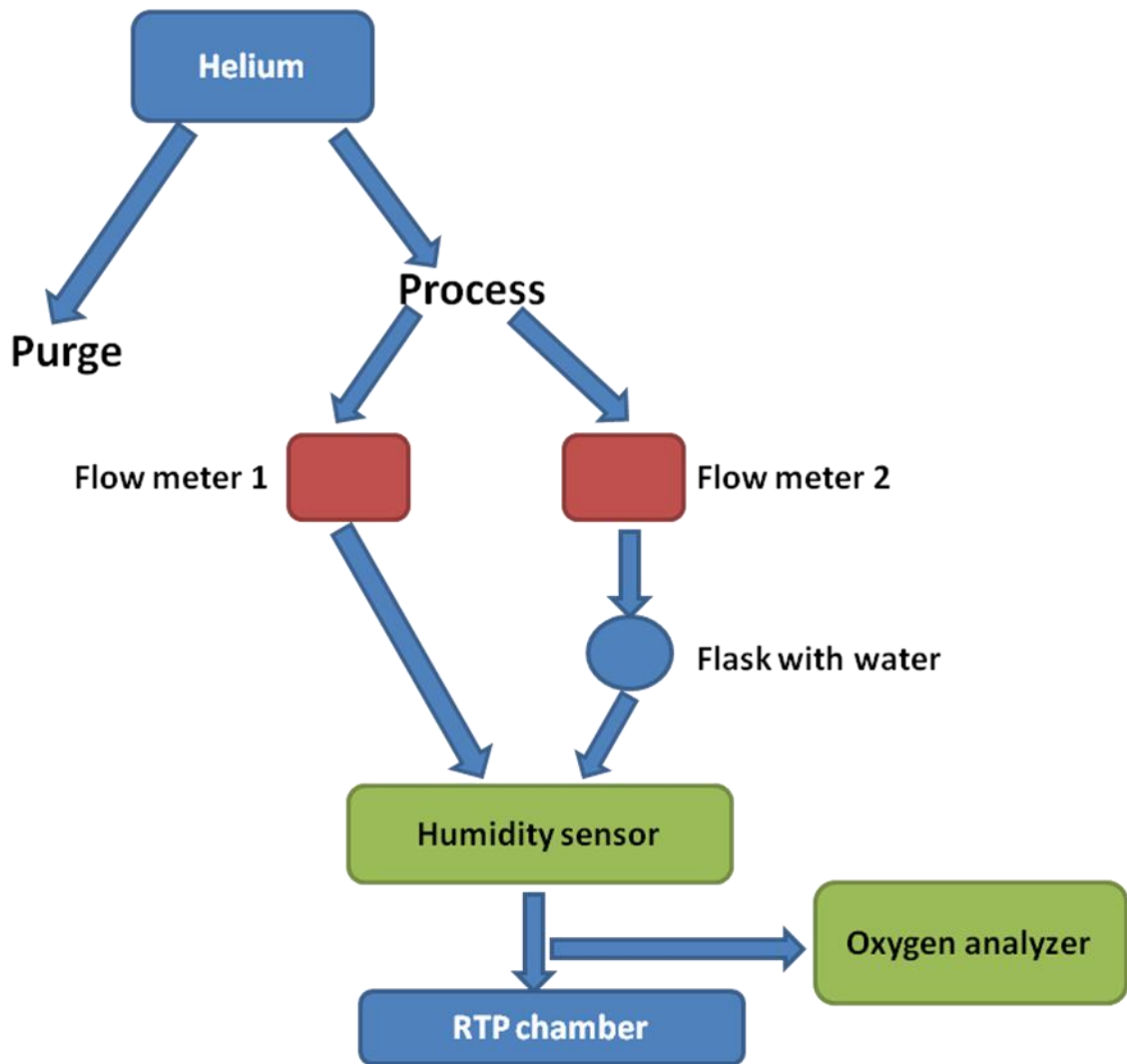


Figure 4.1. Gas route to test moisture effect on heat treatment.

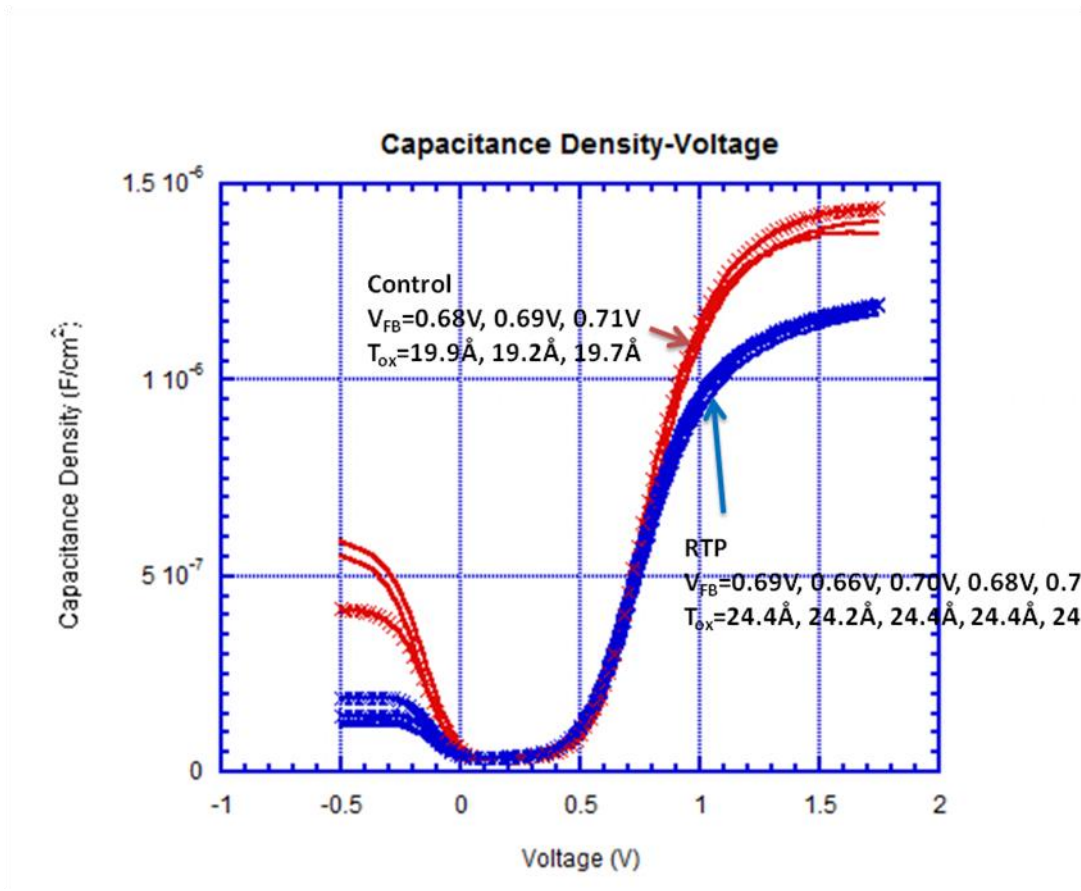


Figure 4.2. Capacitance density-voltage characteristics of n-type MOS capacitors before and after rapid thermal process with moisture exists, flatband voltages and EOTs extracted from the characteristics are marked.

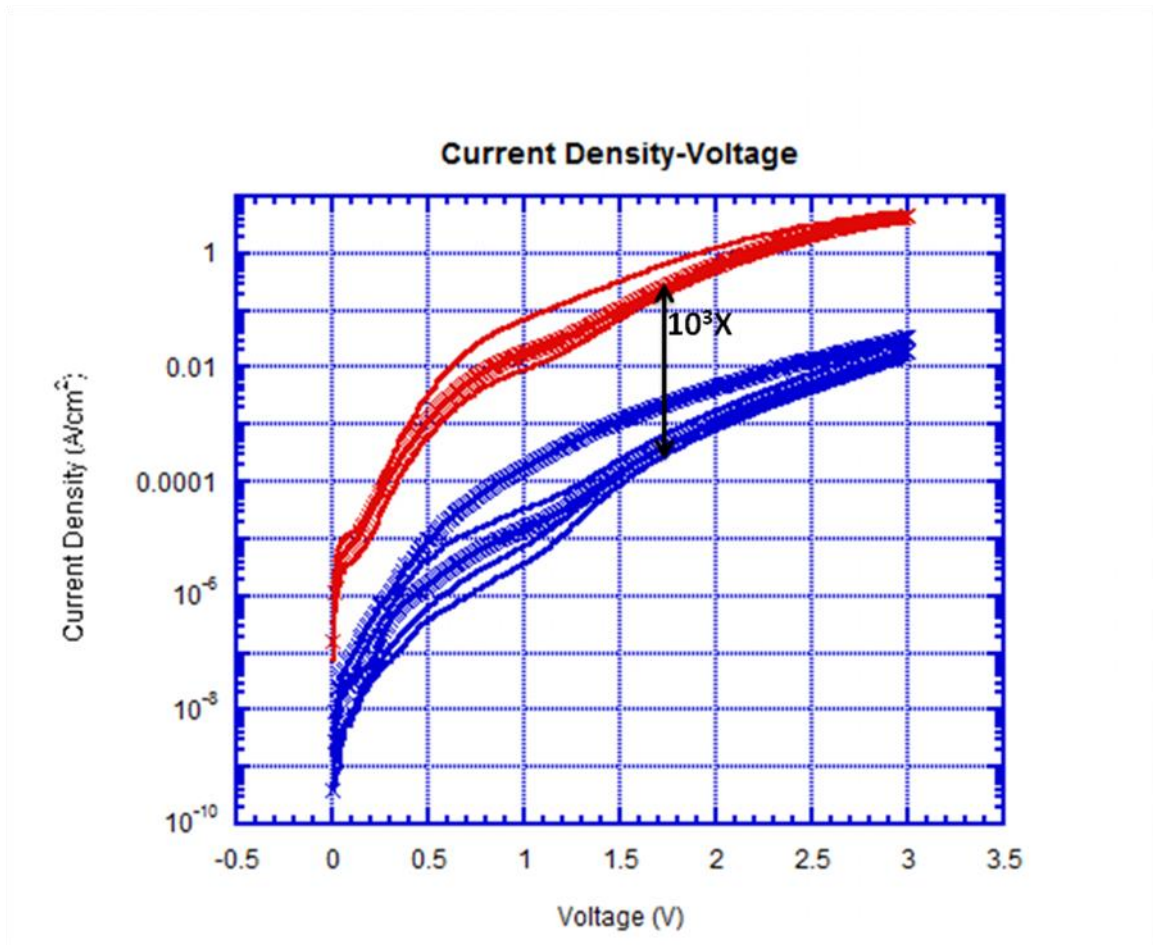


Figure 4.3. Current density-voltage characteristics of n-type MOS capacitors before and after rapid thermal process with moisture exists.

Chapter 5 Lateral Heating Process Experiments and Results

5.1 Background

At the beginning of the exploratory process, a 4'' Si wafer was used in the RTP as the substrate, and the test sample, which was a quarter of the 2'' Si wafer, was put onto the substrate. The temperature was raised to 1050 °C~1080 °C, and the holding time was in the range of 10 seconds~4 minutes, changing depending on the thickness of the SiO₂ layer. Later we observed this specific trend: after several RTP heating processes, the 4'' Si substrate got bent near the centre point, making it convex, and the test sample was just supported by the peak point of the substrate. The sample edge regions were suspending above the substrate, and the MOS capacitors gate leakage current reduction is more likely to be found in these hanging regions. The structure schematic is shown in figure 5.1.

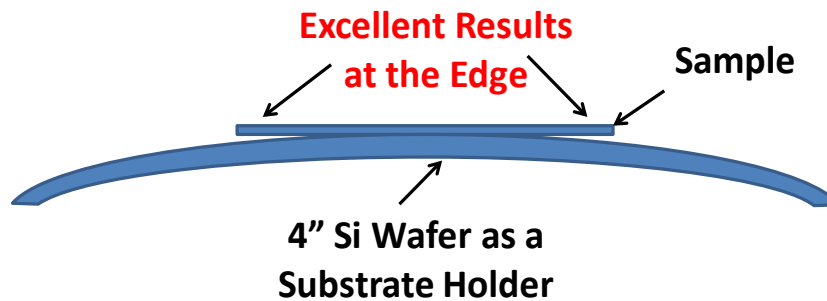


Figure 5.1. Special condition when obvious gate leakage current reduction could be available. After several times' RTP, the 4'' Si substrate became convex, and the good results are available in the sample's hanging edges.

The first assumption for explaining this phenomenon was that the cooling rate at the hanging edges might be faster, which could brought structure changes. Dr. Chen and his students found that a smaller Si substrate results a faster cooling rate. By changing the

size of the Si substrate, they found out that once the cooling rate reaches 50 °C/sec, which could be easily achieved with the 4'' Si substrate, there is no obvious improvement. The cooling rate could not be a crucial factor for the good results at the hanging edges.

The second assumption was that the vertical non-uniform heating could brought structure changes, and the sample's surface heating is supposed to be more than the inner bulk heating. We applied the flash lamp annealing (FLA) on the samples. Since the FLA is a vertically non-uniform heating only in milliseconds, it is able to heat only at the sample surface, in a depth ranging from tens of micrometers to a few hundreds of micrometers. Again, there is no obvious improvement comparing with the control sample. The vertical non-uniform heating could not be a crucial factor, either.

The third assumption was that the lateral heat flow from the center contact region to the hanging edge region might cause structure changes. To prove this hypothesis, several experiments were designed, trying to imitate the hanging structure in figure 6.1, and to enable better heat flow from contact region to hanging edge region. The results of these experiments helped us to understand the underlying mechanism of the leakage current reduction phenomenon.

5.2 Effect of Direct Hanging and Heat Transportation

Based on the assumption that the key factor which brings the appealing electrical properties is the lateral heating from the contact region of the sample to the hanging edge region, a large enough heat flow must be guaranteed to arrive at the sample contact region.

Meanwhile, if the sample does not have any other heat source, the heat arrives at the contact region will definitely flow towards the hanging region. Thus the two requirements for the RTP system are achieved: enough heat on the sample contact region, and no other heat source for the whole sample.

If we could block the light radiation from the top of the RTP chamber, there would be no other heat source for the sample, since sample does not directly receive any light. This could be simply achieved by putting a 4'' Si wafer above the quartz chamber.

If a step structure could be etched on the 4'' Si substrate, the sample could be directly hanged over the step. In this situation, only one contact interface for the heat flow exists. More heat generated on the 4'' Si substrate would arrive at the sample contact region. Si could be etched with tetramethylammonium hydroxide (TMAH) solution, and SiO₂ is a perfect material for etching mask^{[54][55][56]}. SiO₂ could be easily patterned with traditional photolithography and HF etching. The schematic for this procedure is shown in figure 5.2.

The improved lateral heating process positioning is illustrated in figure 5.3. The heat originates from the 4'' Si substrate, and directly flows into the hanging sample. Satisfactory lateral heating flow is now under control.

Ultrathin silicon oxide samples are thermally grown as stated in 2.2. The lateral heating process was executed in N₂ and O₂ mixture environment. One sample was processed at

1080°C for 10 seconds, and the other sample was processed at 1100°C for 10 seconds. Both of the samples went through a temperature increase rate of 10°C/second. For 1080°C sample, the O₂ concentration was between 220 ppm to 250 ppm; for 1100°C sample, the O₂ concentration was around 195 ppm.

The control sample, which means silicon oxide which did not go through heat treatment, has an equivalent oxide thickness (EOT) of 28.82Å, and the gate leakage current density is 0.07A/cm². This gate leakage current density is higher than simulated gate leakage current density of the ideal SiO₂ with similar thickness, and we assume contamination as the reason. The flatband voltage shift of the control sample from the ideal value also supports this assumption.

After lateral heating process, both of the silicon oxide samples got regrowth. The regrowth was 3-4Å in hanging region, and 0-1Å in contact region. According to ideal SiO₂ gate leakage current density simulation, 3-4Å increase in thickness corresponds to 1.5 to 2 order of magnitude leakage current density reduction^[16].

The capacitance density-voltage (CV) and current density-voltage (IV) curves of the MOS capacitors are exhibited in figure 5.4 and 5.5. From the IV curve, it is obvious that there is huge gate leakage current density reduction after heat treatment. Part of the reason is that the heat treatment improves silicon oxide quality, and gets rid of contamination. Comparing the gate leakage current density with ideal simulation value, there is still 1-2 order of magnitude reduction, which is believed to be introduced by the lateral heat-

ing process.

However, the gate leakage current density reduction is not uniform. From the experiment results, there is not any principle which shows how the locations of MOS capacitors with appealing electrical properties distribute among the whole sample. Gate leakage current density reduction phenomenon just appears randomly. This implies the lateral heating effect is not uniform with this experiment condition. The reason might be: the light radiation comes from bottom linear tungsten-halogen lamps is reflected by surfaces inside RTP chamber, in this way, some light could still arrive at sample surface, which provides an energy source, and could be a disturbance to the lateral heat flow from contact region to hanging region.

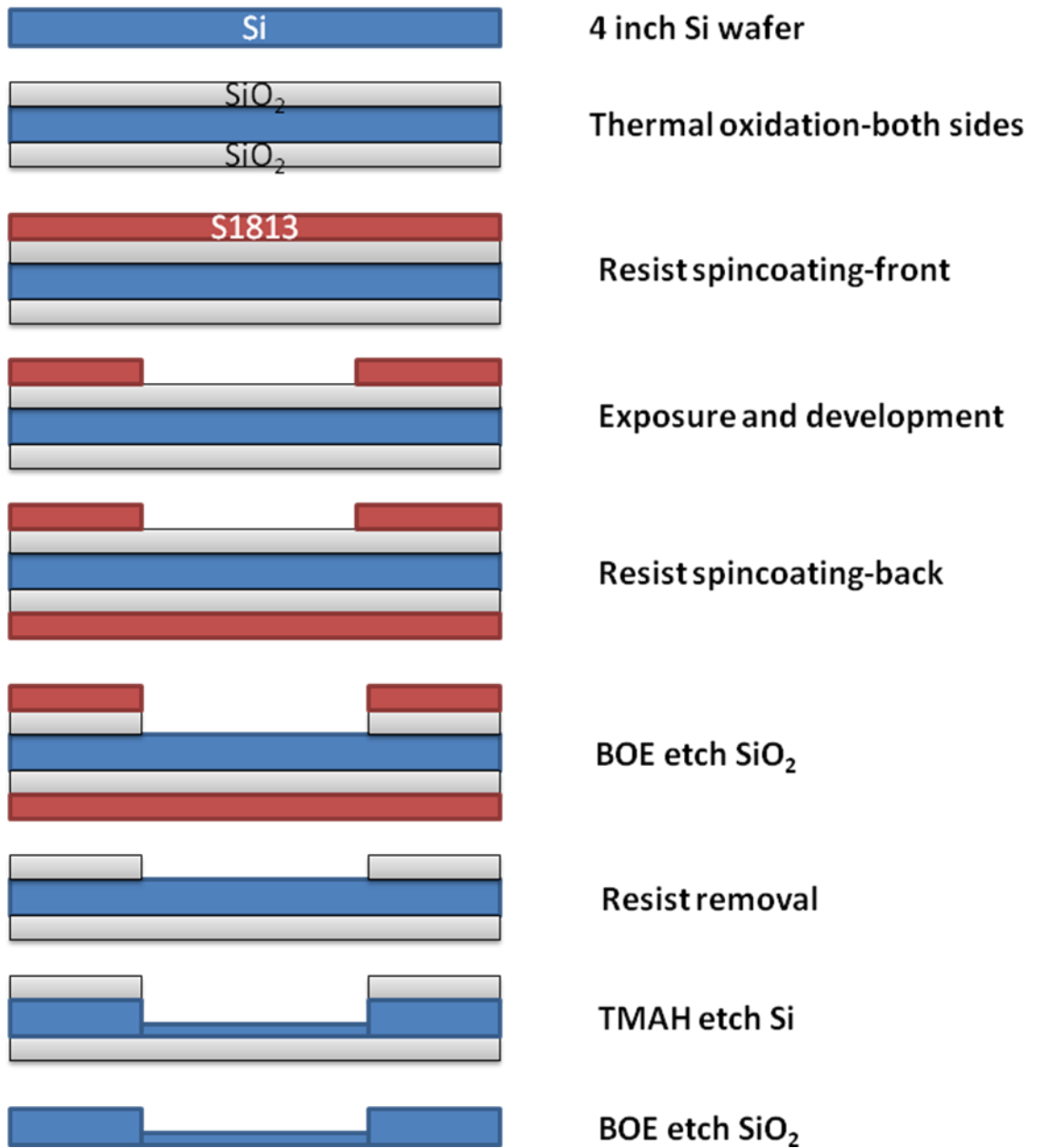


Figure 5.2. The schematic of Si step structure etching by TMAH.

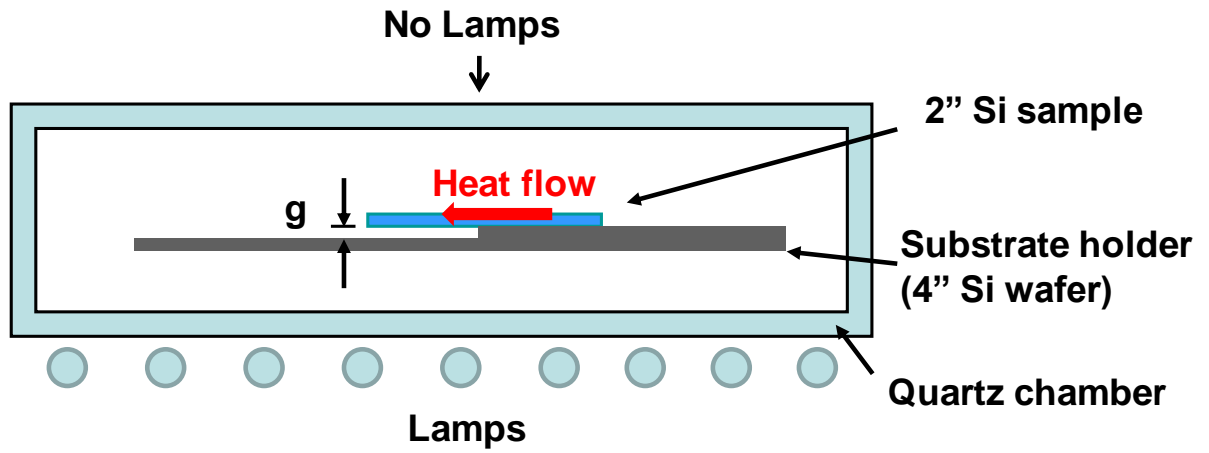


Figure 5.3. Modification of the existing Modular Process Technology Corp. model RTP-600S system. Direct hanging and large lateral heat flow could be easily achieved with this structure.

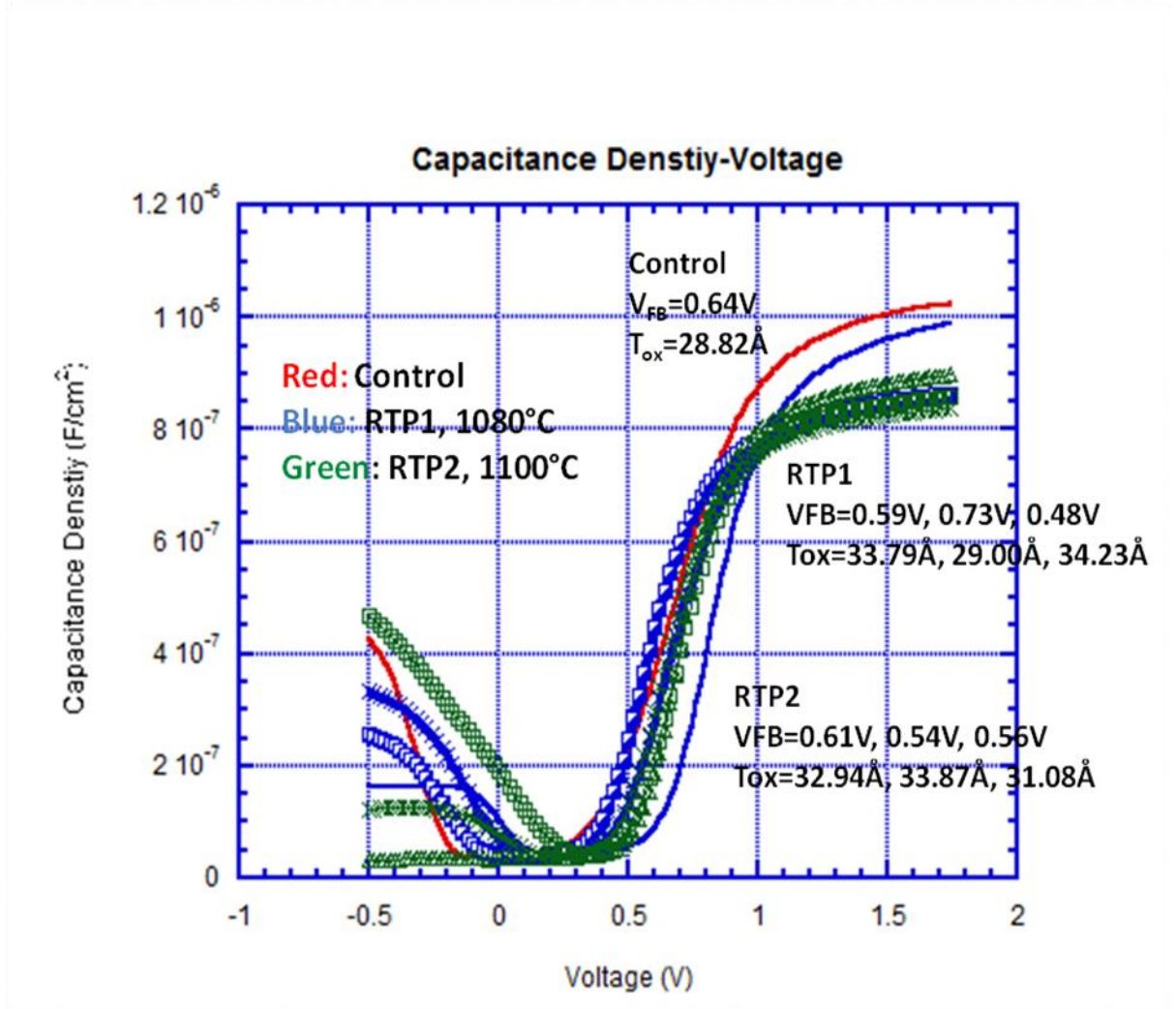


Figure 5.4. Capacitance density-voltage characteristics of n-type MOS capacitors before and after lateral heating process with a substrate step structure, flatband voltages and EOTs extracted from the characteristics are marked.

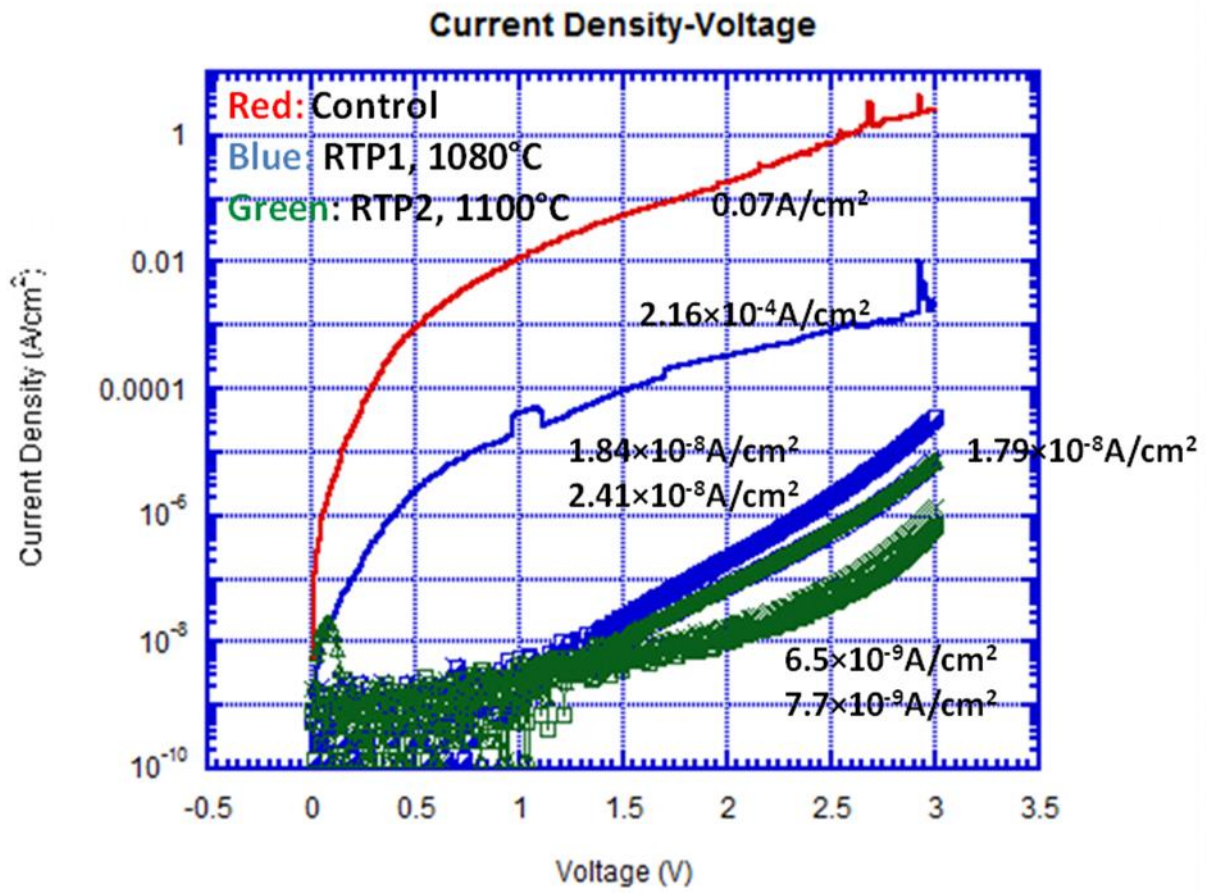


Figure 5.5. Current density-voltage characteristics of n-type MOS capacitors before and after lateral heating process with a substrate step structure, gate leakage current densities at $V=V_{FB}+1$ are marked.

5.3 Effect of Sandwich Structure

To prove the hypothesis that the lateral heat flow from the center contact region to the hanging edge region might cause the appealing phenomenon, Dr. Chen designed a sandwich structure to control the lateral heating process, the top view and the side view of this structure is shown in figure 5.6. A quarter piece of the 2'' Si wafer acted as the sample support, being named Si support 1, and it was put directly above the 4'' Si substrate. The sample was cut into a rectangular shape, and it was put above the Si support 1, with the edge region hanging up. A long narrow Si piece was put above the center of the sample, acting as the support for the radiation blocker, with the name Si support 2. The radiation blocker was also a rectangular piece of Si just a little larger than the sample; it blocked all the top light radiation from the sample. In this structure, the sample was thoroughly isolated from the radiation, all the heat came from heat transportation between the directly contacted Si wafers.

The amount of heat, thus the temperature of the Si wafers should be dependent on the area exposed to light radiation, the larger the area is, the higher the temperature should be. It was assumed that the 4'' Si substrate should have the highest temperature and the most heat quantity, which is then transported to the sample. Some heat could also be transported to the radiation blocker through the Si support 2. This assumption was verified by the thermocouples. It was measured that when the substrate temperature was 1090 °C, the sample temperature was 1050 °C, and the radiation blocker temperature was just 1030 °C, the assumption is correct. The heat flow is illustrated in figure 5.6, the side view of the sandwich structure. The lateral heating in the sample from the center contact

region to the hanging edge region is realized.

The lateral heating process was executed in He and O₂ mixture environment, while the O₂ concentration was maintained around 195 ppm. The dew point value was -54.2°C, which means the humidity was low enough that it would not bring any regrowth effect. The sample's position in the RTP chamber during the lateral heating process was the same with that displayed in figure 6.6. The lateral heating was processed at 1060°C for 10 seconds, and the temperature increase rate was 10 °C/second.

There was no obvious SiO₂ thickness increase after the lateral heating process. As marked in figure 5.7, the EOT for the 3 control devices are 23.4Å, 22.9Å, and 22.2Å; the EOT for the LHP device near the contact region is 23.3Å; the EOT for the 3 LHP devices in the hanging region are 22.4Å, 23.2Å, and 23.7Å. With this limitation of the SiO₂ regrowth, which was achieved by precise control of the O₂ concentration, all the leakage current reduction could be attributed to lateral heating process effect.

There is a correlation between the flatband voltage shift and the leakage current reduction is clearly illustrated in figure 5.7 and 5.8. The flatband voltages of the 3 control devices serve as the reference flatband voltages, and the values are 0.65V, 0.68V, and 0.71V. The deviation from the theoretically calculated flatband voltage (0.85V) is assigned to the contamination during the fabrication process. The flatband voltage of the LHP device near the contact region is 0.38V, with a slight shift toward the negative direction comparing to the control devices. The flatband voltages of the 3 LHP devices in the

hanging region are 0.19V, 0.2V and 0.22V, with more shifts toward the negative direction. Gate leakage current density of these devices are recorded at $V=V_{FB}+1$, and the results for the 3 control devices are $1.06\text{A}/\text{cm}^2$, $0.13\text{A}/\text{cm}^2$ and $0.13\text{A}/\text{cm}^2$, which match well with the simulated gate leakage current density of the ideal SiO_2 with similar thickness. The result of the LHP device near the contact region is $0.01\text{A}/\text{cm}^2$, which is 1 to 2-order-of-magnitude reduction comparing to the control devices; the results of the 3 LHP devices in the hanging region are $3.7 \times 10^{-6}\text{A}/\text{cm}^2$, $1 \times 10^{-6}\text{A}/\text{cm}^2$ and $1.2 \times 10^{-6}\text{A}/\text{cm}^2$, which are 4 to 5-order-of-magnitude reduction comparing to the control devices. It has been illustrated that no gate leakage current reduction is caused by the increase of the SiO_2 thickness; the results are thoroughly attributed to the lateral heating process effect.

An attracting correlation is shown in figure 5.7 and 5.8 that there is always flatband voltage (V_{FB}) shift after lateral heating process, and the more flatband voltage shift, the more gate leakage current reduction. We assume this as the fundamental mechanism for the lateral heating process effect. The analysis of Si substrate structure and work function change should be further explored. It has been reported that strained Si formats near the SiO_2/Si interface after thermal oxidation in furnace^{[53][57][58][59]}, and the tensor strained Si was caused by the compress stress in the SiO_2 transition layer near the interface^[53]. In the transition layer, the SiO_2 network is believed to be compressed due to a large volume expansion upon oxidation^{[60][61]}. In furnace oxidation process, the temperature is slowly increased, and naturally decreased, which may relax most of the stress. In rapid thermal process, the temperature is increased and decreased much faster. This may build more stress, so the strained Si effect is possible to be strengthened.

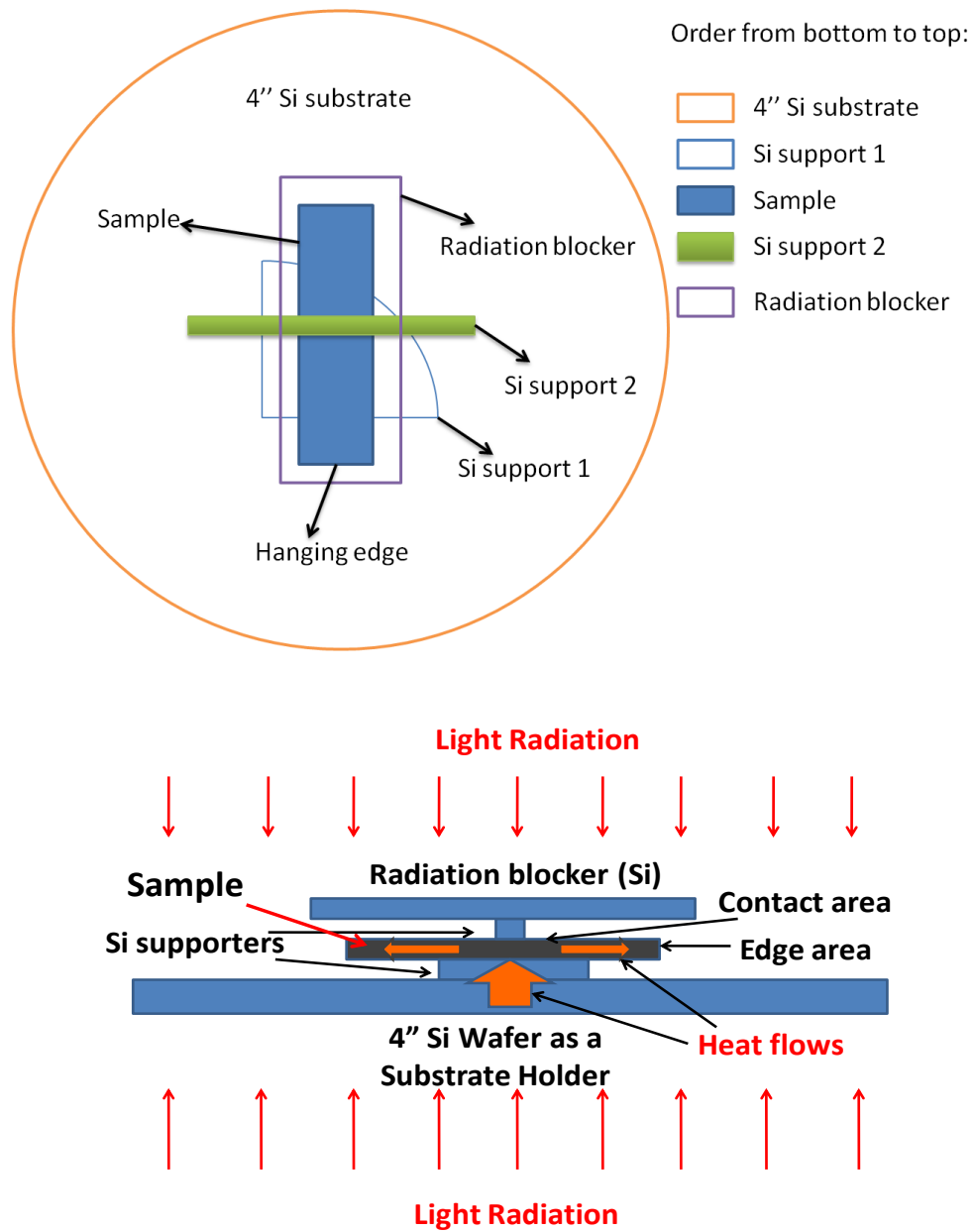


Figure 5.6. The top view (above) and the side view (bottom) of the RTP sandwich structure. MOS capacitors gate leakage current great reduction is observed in the hanging edge region.

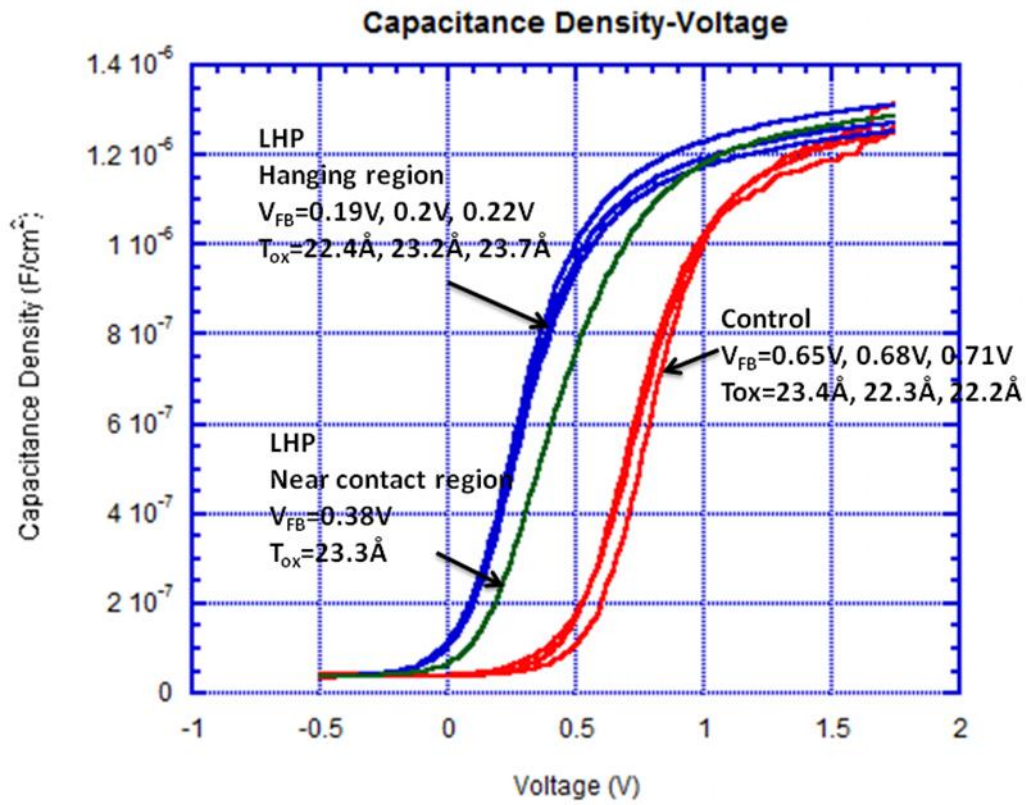


Figure 5.7. Capacitance density-voltage characteristics of the n-type MOS capacitors before and after lateral heating process, flatband voltages and EOTs extracted from the characteristics are marked.

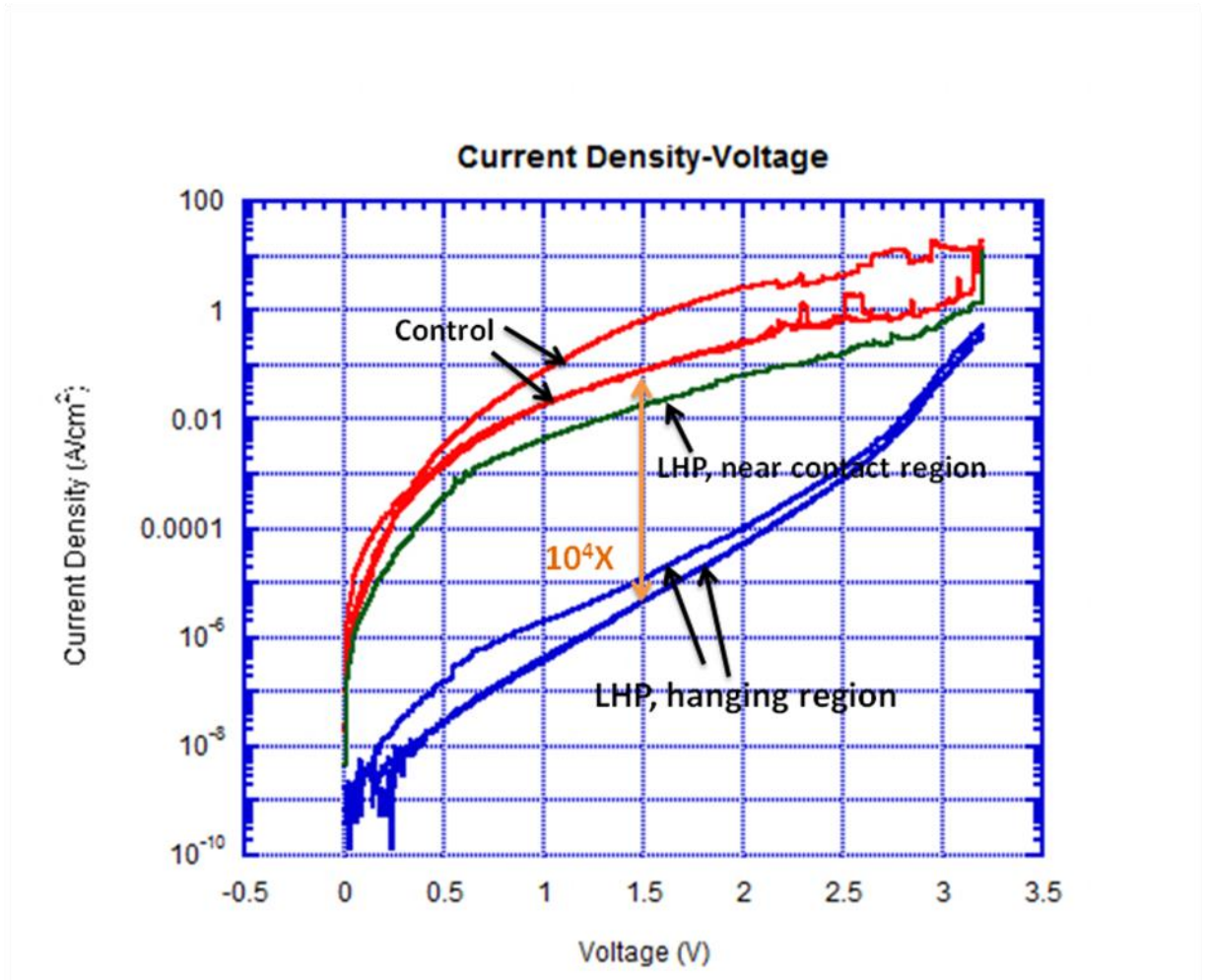


Figure 5.8. Current density-voltage characteristics of the same MOS capacitors. There is 4 to5-order-of-magnitude gate leakage current reduction after the lateral heating process.

Chapter 6 Conclusion and Future Work

6.1 Conclusion

An appealing improvement of MOS capacitors electrical property has been achieved. By applying lateral heating process on Si wafer with thermally grown ultrathin SiO₂ (~20Å), the gate leakage current density of MOS capacitors could be reduced by 3-5 order of magnitude. Since unacceptable gate leakage current is one of the main reasons which prevent the scaling development trend in semiconductor industry, this technology brings a possibility to postpone the end of scaling trend, and pave a way for extensive application in industry.

The underlying mechanism of this appealing phenomenon has been explored. After lateral heating process, the flatband voltage of MOS capacitors shifts to negative direction. This is probably due to strained Si at the SiO₂/Si interface, which is induced by the compress stress in the SiO₂ transition layer. Rapid increasing and decreasing of temperature in RTP prevent the stress relaxation, and strengthen the effect.

A new method for patterning of MOS capacitors metal gate has been developed, and lift-off process has been replaced by wet etching process. This method provides better contact between dielectric layer and metal gate, meanwhile the operation is much easier.

6.2 Future Work

Dielectric materials with higher dielectric constants (high-k materials) have already over-

came SiO₂ and became the dominant dielectric materials in semiconductor field. Since the underlying mechanism for our appealing finding might be Si structure change, not SiO₂ structure change, it is reasonable to assume that this effect could be applied on high-k gate oxide stacks to reduce the gate tunneling leakage current. In the future, it is valuable to demonstrate the validity of the lateral heating process for improving the high-k gate oxide stacks comparable to those in industry. If the validity could be proved, this technology would be able to further improve the properties of the silicon MOS devices, and pave a way for extensive application of this technology in industry.

Reference

- [1] I. M. Ross, "The invention of the transistor," *proceedings of the IEEE*, vol. 86, no. 1, pp. 7-28, 1998.
- [2] W. Shockley, *Electrons and Holes in Semiconductors*. New York: Van Nostrand, 1950.
- [3] D. Kahng and M. M. Attala, "Silicon-Silicon Dioxide Surface Device," *IRE Device Research Conference, Pittsburg*, 1960.
- [4] G. E. Moore, "Cramming more components onto integrated circuits," *Electronics*, pp. 113-117, April 19, 1965.
- [5] G. E. Moore, "Progress in digital integrated electronics," *International Electron Device Meeting*, IEEE, pp. 11-13, 1975.
- [6] Wikipedia, Moore's Law, http://en.wikipedia.org/wiki/Moore's_law.
- [7] *The International Technology Roadmap for Semiconductors (ITRS)*, 2010 edition.
- [8] D. L. Critchlow, "MOSFET scaling-the driver of VLSI technology," *IEEE Proc.*, vol. 87, pp. 659, 1999.
- [9] J. Singh, *Semiconductor Devices: Basic Principles*. New York: John Wiley & Sons, 2001.
- [10] R. H. Dennard, F. H. Gaensslen, etc, "Design of ion-implanted MOSFETs with very small physical dimensions," *IEEE J. Solid-State Circuits* SC-9, pp. 256-268, 1974.
- [11] W. Haensch, E. J. Nowak, etc, "Silicon CMOS devices beyond scaling," *IBM Journal of Research and Development*, vol. 50, no. 4/5, pp. 339-361, 2006.
- [12] S. Thompson, P. Packan, etc, "Mos scaling: transistor challenges for the 21st century," *Intel Technol. J.*, Q3, 1998.
- [13] "Technology backgrounder: high-k gate oxides", icknowledge.com.
- [14] K. Roy, S. Mukhopadhyay, etc, "Leakage current mechanisms and leakage reduction techniques in deep-submicrometer CMOS circuits," *proceedings of the IEEE*, vol. 91, no.2, pp. 305-327, 2003.
- [15] Pang Leen Ong, "Phonon-energy-coupling-enhancement effects and its application," PhD dissertation, University of Kentucky, 2008.
- [16] S. H. Lo, D. A. Buchanan, etc, "Quantum-mechanical modeling of electron tunneling current from the inversion layer of ultra-thin-oxide nMOSFET's," *IEEE Electron Device Letters*, vol. 18, pp. 209-211, 1997.
- [17] G. D. Wilk, R. M. Wallace, etc, "High-k gate dielectrics: current status and materials properties consideration," *Applied Physics Review*, vol. 89, num. 10, pp. 5243-5275, 2001
- [18] K. Henson, H. Bu, etc, "Gate length scaling and high drive currents enabled for high performance SOI technology using high-k/metal gate," *IEDM*, pp. 645-648, 2008.
- [19] M. Takahashi, A. Ogawa, etc, "Gate-first processed FUSI/HfO₂/HfSiO_x/Si MOSFETs with EOT=0.5 nm," *IEDM*, pp. 523-526, 2007.
- [20] T. Ando, M. M. Frank, etc, "Ultimate EOT scaling (< 5Å) using Hf-based high-k gate dielectrics and impact on carrier mobility," *ECS Transactions*, vol. 28, no. 1, pp. 115-123, 2010.
- [21] B. Hoeneisen, C. A. Mead, "Fundamental limitations in microelectronics-I. MOS technology," *solid state electronics*, vol. 15, pp. 819-829, 1972.
- [22] J. T. Wallmark, "Fundamental physical limitations in integrated electronic circuits,"

- Inst. Phys. Conf. Ser.*, No. 25, pp. 133-167, 1975
- [23] C. Hu, "Gate oxide scaling limits and projections," *IEDM tech. Digest*, pp. 96-99, 1996.
- [24] J. H. Stathis, D. J. Dimaria, "Reliability projection for ultra-thin oxides at low voltage," *IEDM tech. Digest*, pp. 167-170, 1998.
- [25] L. Chang, Y. Choi, etc, "Extremely scaled silicon nano-CMOS devices," *Proceedings of the IEEE*, vol. 91, no. 11, pp. 1860-1873, 2003.
- [26] M. Kanellos, "Intel scientists find wall for Moore's Law," *CENT*, December 01, 2003.
- [27] I. Vurgaftman, J. R. Meyer, etc, "Band parameters for III-V compound semiconductors and their alloys," *Journal of Applied Physics*, vol. 89, no. 11, pp. 5815-5875, 2001.
- [28] S. Iijima, "Helical microtubules of graphitic carbon," *Nature*, vol. 354, pp. 56-68, 1991.
- [29] P. Avouris, "Supertubes," *IEEE spectrum*, vol. 41, no. 8, pp. 40-45, 2004.
- [30] N. S. Hush, "An overview of the first half-century of molecular electronics," *Annals of the New York Academy of Sciences*, vol. 1006, issue 1, pp. 1-20, 2003.
- [31] S. A. Wolf, D. D. Awschalom, etc, "Spintronics: a spin-based electronics vision for the future," *Science*, vol. 294, pp. 1488-1495, 2001.
- [32] K. K. Likharev, "Single-electron devices and their applications," *Proceeding of the IEEE*, vol. 87, no. 4, pp. 606-632, 1999.
- [33] J. W. Lyding, K. Hess, etc, "Reduction of hot electron degradation in metal oxide semiconductor transistors by deuterium processing," *Applied Physics Letters*, vol. 68, pp. 2526-2528, 1996.
- [34] P. J. Chen, R. M. Wallace, "Examination of deuterium transport through device structure," *Applied Physics Letters*, vol 73, pp. 3441-3443, 1998.
- [35] R. A. B. Devine, J. L. Autran, etc, "Interfacial hardness enhancement in deuterium annealed 0.25 μm channel metal oxide semiconductor transistors," *Applied Physics Letters*, vol 70, pp. 2999-3001, 1997.
- [36] C. G. Van de Walle, W. B. Jackson, "Reduction of hot electron degradation in metal oxide semiconductor transistors by deuterium processing-comment," *Applied Physics Letters*, vol. 69, pp. 2441, October, 1996.
- [37] J. H. Wei, M. S. Sun, etc, "A possible mechanism for improved light-induced degradation in deuterated amorphous silicon alloy," *Applied Physics Letters*, vol. 71, pp. 1498-1500, 1997.
- [38] Z. Chen, J. Guo, etc, "Evidence for energy coupling from the Si-D vibration mode to the Si-Si and Si-O vibration modes at the SiO₂/Si interface," *Applied Physics Letters*, vol. 83, pp. 2151-2153, 2003.
- [39] Z. Chen, J. Guo, "Dramatic enhancement of phonon energy coupling at the SiO₂/Si interface due to rapid thermal processing of the gate oxide," *presentation at the 35th IEEE Semiconductor Interface Specialists Conf.*, San Diego, CA, December 9th-11th, 2004.
- [40] Z. Chen, J. Guo, and F. Q. Yang, "Phonon-energy-coupling enhancement: strengthening the chemical bonds of the SiO₂/Si system," *Applied Physics Letters*, vol. 88, pp. 082905, 2006.
- [41] Z. Chen, J. Guo, "Dramatic reduction of gate leakage current of ultrathin oxides through oxide structure modification," *Solid-State Electronics*, vol. 50, pp. 1004-1011,

2006.

- [42] Z. Chen, "Mechanism for generation of the phonon-energy-coupling enhancement effect for ultrathin oxides on silicon," *Applied Physics Letters*, vol. 91, pp. 223513, 2007.
- [43] Z. Chen, J. Guo, and P. Ong, "Fundamental mechanisms for reduction of leakage current of silicon oxide and oxynitride through RTP-induced phonon-energy coupling," *Proc. 14th annual IEEE international conference on advanced thermal processing of semiconductors – RTP2006*, Kyoto, Japan, October 10th-13th, 2006 (invited).
- [44] P. Ong, Z. Chen, "Evidence of enhanced phonon-energy coupling in SiO₂/Si," *Applied Physics Letters*, vol. 90, pp. 113516, 2007.
- [45] T. H. Hou, J. Gutt, etc, "Improved scalability of high-k gate dielectrics by using Hf-Aluminates," *Electrochemical Society Meeting*, Salt Lake City, Utah, Abstract No. 384, 2002.
- [46] W. Kern, D. A. Putotinen, "Cleaning solutions based on hydrogen peroxide for use in silicon semiconductor technology," *RCA Review*, vol. 31, pp. 187, 1970.
- [47] W. Kern, "Handbook of Semiconductor Wafer Cleaning Technology," *William Andrew Publishers*, 1993.
- [48] B. E. Deal, A. S. Grove, "General relationship for the thermal oxidation of silicon," *Journal of Applied Physics*, vol. 36, issue 12, pp. 3770-3778, 1965.
- [49] P. L. Ong, Z. Chen, etc, "Large leakage-current reduction of ultrathin industrial SiON wafers induced by phonon-energy-coupling enhancement." *Electrochem. Solid-State Letters*, vol. 11, no. 11, pp. 293-295, 2008.
- [50] Z. Chen, P. L. Ong, etc, "Reliable observation of large leakage-current reduction of thin SiO₂ induced by phonon-energy-coupling enhancement: problems and solution," *J. Electrochem. Soc.*, vol. 157, pp. 44-48, 2010.
- [51] Wet Etching Recipes, http://www.siliconfareast.com/etch_recipes.htm
- [52] K. R. Williams, K. Gupta, etc, "Etch rates for micromachining processing-part 2," *Journal of Microelectromechanical Systems*, vol. 12, no. 6, pp. 761-778, 2003.
- [53] K. Nakajima, M. Suzuki, etc, "Lattice Distortion at SiO₂/Si(001) interface studied with high-resolution Rutherford backscattering spectroscopy/channeling," *Japanese Journal of Applied Physics*, vol. 45, no. 4A, pp. 2467-2469, 2006.
- [54] J. T. L. Thong, W. K. Choi, etc, "TMAH etching of silicon and the interaction of etching parameters," *Sensors and Actuators A*, vol. 63, pp. 243-249, 1997.
- [55] P. H. Chen, H. Y. Peng, etc, "The characteristic behavior of TMAH water solution for anisotropic etching on both silicon substrate and SiO₂ layer," *Sensors and Actuators A*, vol. 93, pp. 132-137, 2001.
- [56] K. Biswas, S. Kal, etc, "Etch characteristics of KOH, TMAH and dual doped TMAH for bulk micromachining of silicon," *Microelectronics Journal*, vol. 37, pp. 519-525, 2006.
- [57] Y. P. Kim, S. K. Choi, etc, "Direct observation of Si lattice strain and its distribution in the Si(001)-SiO₂ interface transition layer," *Applied Physics Letters*, vol. 71, pp. 3504-3506, 1997.
- [58] N. V. Nguyen, D. ChandlerHorowitz, etc, "Spectroscopic ellipsometry determination of the properties of the thin underlying strained Si layer and the roughness at SiO₂/Si interface," *Applied Physics Letters*, vol. 64, pp. 2688-2690, 1994.
- [59] W. Daum, H. -J. Krause, etc, "Identification of strained silicon layers at Si-SiO₂ interfaces and clean Si surface by nonlinear optical spectroscopy," *Physical Review Letters*,

vol. 71, no. 8, pp. 1234-1237, 1993.

[60] Y. Sugita, S. Watanabe, etc, "Structural fluctuation of SiO₂ network at the interface with Si," *Applied Surface Science*, 100/101, pp. 268-271, 1996.

[61] S. Miyazaki, H. Nishimura, etc, "Structure and electronic states of ultrathin SiO₂ thermally grown on Si(100) and Si(111) surfaces," *Applied Surface Science*, 113/114, pp. 585-589, 1997.

Vita

Lei Han was born in Taigu County, Shanxi Province, P. R. China on September 27th, 1985.

Education

August, 2008 --- Present

Ph. D. Student

Department of Electrical and Computer Engineering, University of Kentucky,

September, 2003 --- July, 2007

Bachelor of Engineering

College of Precision Instrument and Opto-Electronics Engineering,

Tianjin University, P. R. China

Bachelor of Management (Minor)

College of Management, Tianjin University, P. R. China

Awards

RCTF (Research Challenge Trust Fund) Research Scholarship, *University of Kentucky*, Lexington, KY, 2011-2012

RCTF (Research Challenge Trust Fund) Fellowship, *University of Kentucky*, Lexington, KY, 2011-2012

3A Student Scholarship, *Tianjin University*, Tianjin, China, 2004-2007

Publications

“The interfacial quality of HfO₂ on silicon with different thicknesses of the chemical oxide interfacial layer”, S.B.Li, L.Han and Z.Chen, *Journal of The Electrochemical Society*, vol. 157, pp221-224, 2010.

“Lateral heating of SiO₂/Si: interfacial Si structure change causing tunneling current reduction”, Z. Chen, P. Ong, Y. Wang, L. Han, *Applied Physics Letter*, vol. 100, pp. 171602 1-4, 2012.